Remote Sensing of Environment 221 (2019) 386–404

Contents lists available at ScienceDirect

Remote Sensing of Environment

journal homepage: www.elsevier.com/locate/rse

Regional differences of lake evolution across China during 1960s–2015 and its natural and anthropogenic causes

Guoqing Zhang[a,b,*], Tandong Yao[a,b], Wenfeng Chen[a], Guoxiong Zheng[a,g], C.K. Shum[c,k], Kun Yang[a,b], Shilong Piao[b,d], Yongwei Sheng[e], Shuang Yi[f], Junli Li[g], Catherine M. O'Reilly[h], Shuhua Qi[i], Samuel S.P. Shen[j], Hongbo Zhang[a], Yuanyuan Jia[c]

[a] Key Laboratory of Tibetan Environmental Changes and Land Surface Processes, Institute of Tibetan Plateau Research, Chinese Academy of Sciences, Beijing 100101, China
[b] CAS Center for Excellence in Tibetan Plateau Earth Sciences, Beijing 100101, China
[c] Division of Geodetic Science, School of Earth Sciences, The Ohio State University, Columbus, OH 43210, USA
[d] Department of Ecology, College of Urban and Environmental Sciences, Peking University, Beijing 100871, China
[e] Department of Geography, University of California Los Angeles, Los Angeles, CA 90095, USA
[f] Department of Natural History Sciences, Hokkaido University, Sapporo 0600808, Japan
[g] Xinjiang Institute of Ecology and Geography, Chinese Academy of Sciences, Urumqi 830011, China
[h] Department of Geography-Geology, Illinois State University, Normal, IL 61790, USA
[i] School of Geography and Environment, Jiangxi Normal University, Nanchang 330022, China
[j] Department of Mathematics and Statistics, San Diego State University, San Diego, CA 92182, USA
[k] Institute of Geodesy and Geophysics, Chinese Academy of Sciences, Wuhan 430077, China

ARTICLE INFO

Keywords:
China's lakes
Lake area change
Climate change
Human activity
Landsat satellite image

ABSTRACT

Lakes are sensitive indicators of anthropogenic climate change and also respond to direct human activities. Yet, long-term lake inventories and quantitative evaluation of the factors driving observed lake changes across China remain elusive. Here, for the first time, we examined multi-decadal lake area changes in China during 1960s–2015, using historical topographic maps and > 3831 Landsat satellite images, including lakes as fine as ≥1 km^2 in size. In addition, we quantified the causes of lake changes from climatic and anthropogenic factors. The total area of lakes in China has increased by 5858.06 km^2 (9%) between 1960s and 2015, and with heterogeneous spatial variations. Lake area changes in the Tibetan Plateau, Xinjiang, and Northeast Plain and Mountain regions reveal significant increases of 5676.75, 1417.15, 1134.87 km^2 (≥15%), respectively, but the Inner-Mongolian Plateau shows an obvious decrease of 1223.76 km^2 (22%). We find that 141 new lakes have appeared predominantly in the arid western China; but 333 lakes, mainly located in the humid eastern China, have disappeared over the past five decades. We conclude that climate factors have played a dominant role in lake changes across China, coupled with noticeable anthropogenic contribution of ~35% in the Eastern Plain and Yunnan-Guizhou Plateau. This study has substantial implications to improve decision support regarding water-resource management strategies and land-use planning throughout China.

1. Introduction

Lakes are sensitive to climate change and to anthropogenic factors such as land use; they therefore act as indicators of various contributors of environmental change (Adrian et al., 2009). Climate-driven fluctuations in lake surface area have been observed in many remote sites in the world. Climate warming has contributed to drying of the Arctic ponds (Smol and Douglas, 2007), and the disappearance of lakes in discontinuous permafrost regions in Alaska and Siberia (Smith et al., 2005). Climate change has driven divergent directions of water body area changes in contiguous United States (Zou et al., 2018). In the Italian Alps, there have been pond surface area reductions due to increased evaporation/precipitation ratio (Salerno et al., 2014). In the Third Pole regions, changes in glacial lakes (Salerno et al., 2016; Zhang et al., 2015), and glacier-fed lakes (Song et al., 2014; Zhang et al., 2017c) are driven by glacier melt and varying patterns of precipitation.

* Corresponding author at: Key Laboratory of Tibetan Environmental Changes and Land Surface Processes, Institute of Tibetan Plateau Research, Chinese Academy of Sciences, Beijing 100101, China.
E-mail address: guoqing.zhang@itpcas.ac.cn (G. Zhang).

https://doi.org/10.1016/j.rse.2018.11.038
Received 24 December 2017; Received in revised form 21 November 2018; Accepted 24 November 2018

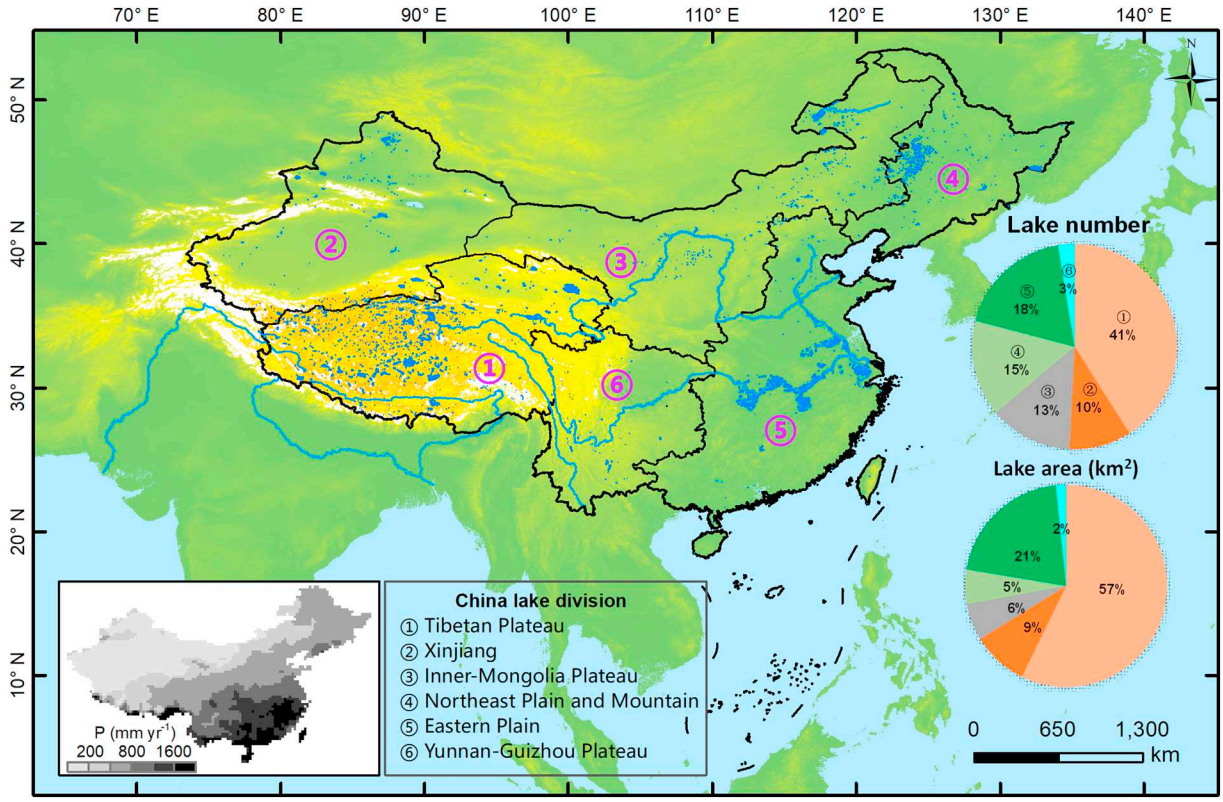

Fig. 1. Geographical distribution of lakes in China. Mountain glaciers and rivers are also shown. Lakes in China are divided into six sub-regions (①–⑥) according to geographical features and climatic differences (Ma et al., 2010). These regions consist of the Tibetan Plateau (TP), Xinjiang (XJ), Inner-Mongolian Plateau (MP), Northeast Plain and Mountain (NE), Eastern Plain (EP), and Yunnan-Guizhou Plateau (YG). The fraction lake number and area (%) in the six sub-regions (①–⑥) are labelled in the pie chart in lower right corner. Inset in the lower left corner displays the mean annual precipitation (P) between 1961 and 2013 from GPCC data, which indicates the arid or humid climate in different geographical regions across China.

In addition, the anthropogenic-driven fluctuations of lakes have been also widely recorded. The shrinking of several of the world's large saline lakes is due to water withdrawals for human use (Wurtsbaugh et al., 2017). The permanent water loss in the Middle East and Central Asia is linked to human activities from river diversion or damming and unregulated withdrawal (Pekel et al., 2016). The intensified human water regulations have accelerated the vulnerability of lakes in the Yangtze Basin, downstream of the Three Gorges Dam (Wang et al., 2014).

Accelerated climate warming (Duan and Xiao, 2015) and rapid economic development in China during the last three decades have exacerbated regional differences in water resources such as the quantity of lakes and wetlands (Ma et al., 2010; Mao et al., 2018; Niu et al., 2012), as well as water quality (Tong et al., 2017). China has a vast area of 9.6 million km^2, with a diverse range of climatic patterns and drastically different levels of economic development. Lakes are abundant but heterogeneously distributed in China (Ma et al., 2011) and represent a critical source of freshwater (Fig. 1). Understanding the large-scale patterns of lake change in China is important for long-term sustainability. Although two lake inventories of China were conducted during 1960–1980 (Wang and Dou, 1998), and again during 2005–2006 (Ma et al., 2010), current lake changes and their drivers are still unknown. Moderate Resolution Imaging Spectroradiometer (MODIS) sensors onboard NASA's Terra/Aqua Earth Observing System (EOS) platforms have also been used to monitor lake changes at high temporal resolution (8-day) during 2000–2010 (Sun et al., 2014), but with a coarse spatial resolution at 250 or 500 m. This is a limitation for monitoring small (~1 km^2) lakes or lakes with little area change, which is the case for most of the lakes across China. Although global surface water maps are available using high-resolution (15 or 30 m) Landsat satellite imagery (Donchyts et al., 2016; Pekel et al., 2016; Verpoorter et al., 2014), tedious visual examination and manual editing are usually required to separate lakes from other water bodies such as rivers, wetlands, or reservoirs (Carroll et al., 2009; Lehner and Döll, 2004; Verpoorter et al., 2014; Yamazaki et al., 2015). Thus, there have been challenges for applying satellite datasets to understand long-term lake changes and at high-resolution scales.

The greatest changes in climate have occurred in recent decades in China (Ma et al., 2015; Wang et al., 2018), and the complexity of interactions between climate and human land use patterns is increasingly being recognized (Piao et al., 2010). There definitely is a need to update the Chinese lake inventory for datasets with finer spatial resolutions, increase its temporal sampling, and lengthen the data record to multiple decades. Using a combination of digitized topographic maps and satellite remote sensing, we generated, for the first time, the evolution of high-resolution (30 m) lake area changes (natural lakes excluding wetlands, reservoirs and rivers) in whole of China, including sizes as small as 1 km^2 during 1960s–2015. We then used this dataset to evaluate the relative contributions from climate change and direct human activities to the long-term trends.

2. Data and methods

2.1. Landsat images used

Our study area across China was divided into six geographical regions, the Tibetan Plateau (TP), Xinjiang (XJ), Inner-Mongolian Plateau (MP), Northeast Plain and Mountain (NE), Eastern Plain (EP), and Yunnan-Guizhou Plateau (YG) according to previous studies (Fig. 1) (Ma et al., 2010; Shi, 1989; Wang and Dou, 1998). Lake changes and their corresponding driving factors were analyzed at sub-regional scale.

Earth's surface water can be mapped from space using multi-temporal Landsat images since 1970s (Pekel et al., 2016), which is the

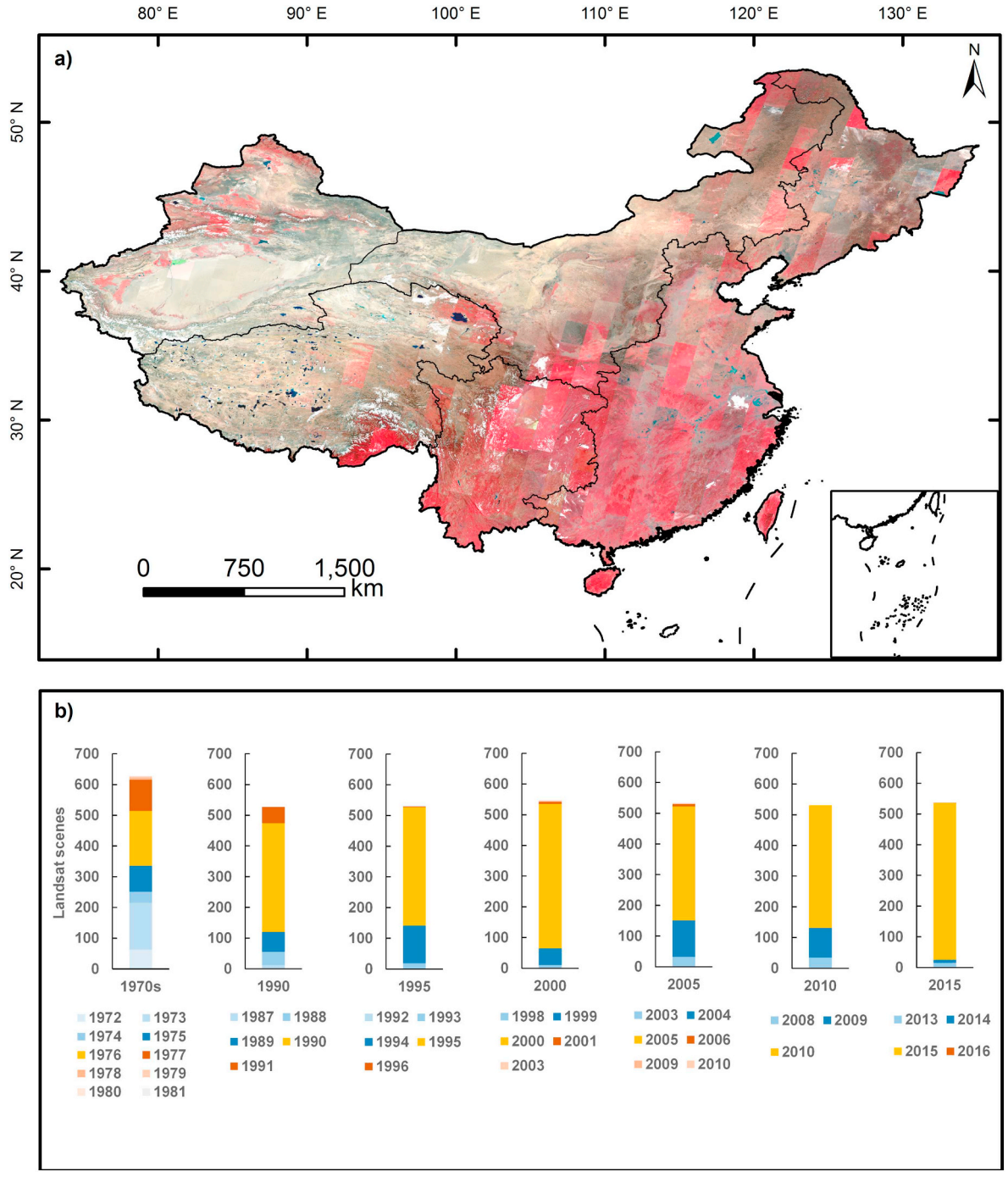

Fig. 2. Landsat data used for lake mapping. a) Mosaicked Landsat-8 OLI imagery in 2015. False color composites of bands 5, 4, 3 are shown. b) Number of Landsat scenes used in the 1970s to 2015. (For interpretation of the references to color in this figure legend, the reader is referred to the web version of this article.)

world's longest and most extensive space-based land observation. Our analysis exploited the Landsat archive (Level 1 Terrain-corrected product) between 1972 and 2015. It includes the Landsat 1–4 multispectral scanner (MSS), Landsat 5 Thematic Mapper (TM), Landsat 7 Enhanced Thematic Mapper-plus (ETM+) and Landsat 8 Operational Land Imager (OLI). The Landsat MSS has a spatial resolution of ~80 m, but it is commonly resampled to 60 m. The other Landsat sensors have the improved spatial resolution of 30 m. At least 516 scenes in each period are needed to cover the whole of China (Fig. 2). Contamination by clouds, especially in the TP with a mean cloud fraction of 45% each day (Yu et al., 2016), led to more images being used to seek cloud-free lake shoreline observations at relative stable seasons (Fig. 3). A total of 3831 scenes (> 2 TB) from 1972 to 2015 were used (Fig. 2b), in addition to further images used in visual inspection and manual editing.

Regional climatic characterization and previous studies (Ma et al., 2010; Shi et al., 2014; Zhang et al., 2017a) allowed definition of the optimal period (with small cloud influence and intra-annual variability) for the six regions: TP (September–November), XJ (August–September), MP (July–September), NE (August–September), EP (August–September), and YG (August–October). Landsat image in a target month was selected first, but the data in other months were also used if a cloud-free image over the lake surface was not available. For example, in the TP, the data in October were the first choice, but September and November might have been selected if there were no available images

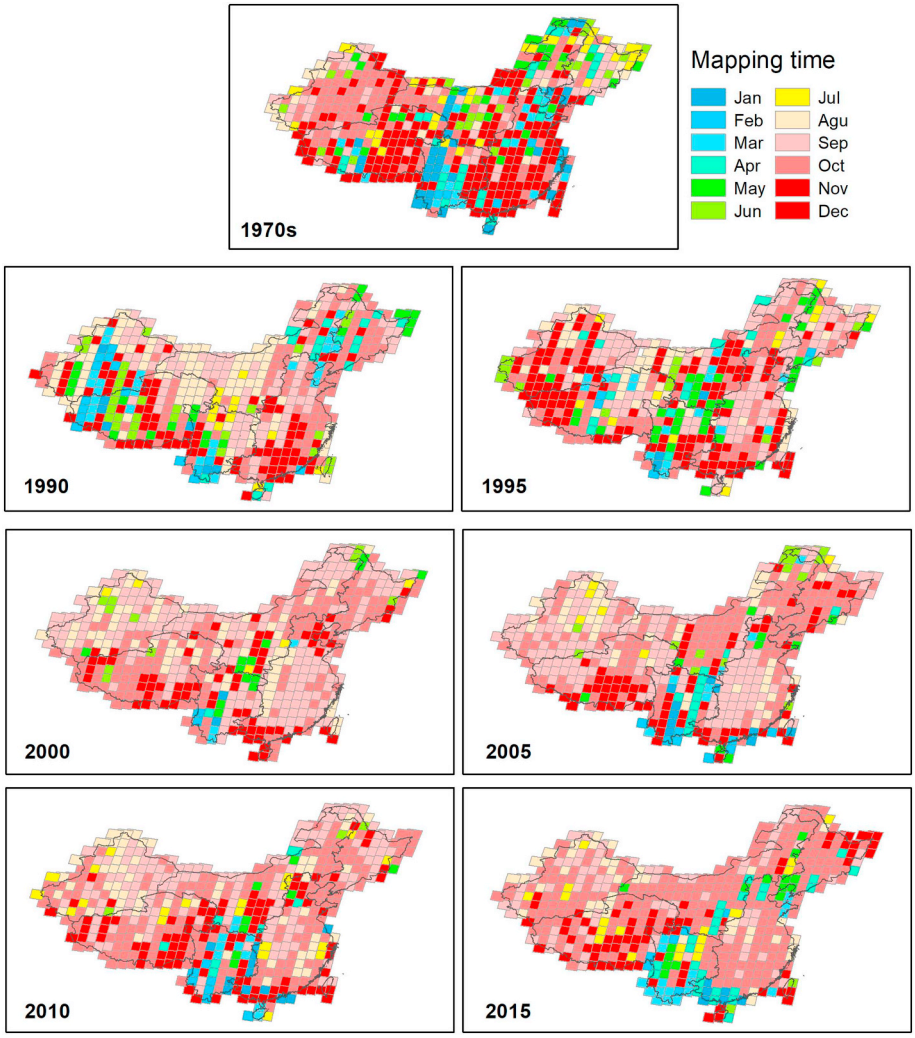

Fig. 3. Optimal mapping months from available Landsat data for different sub-regions in China from the 1970s to 2015.

in October (Fig. 3). Such substitutions occurred more frequently in the period from 1972 to 1990 because there were fewer images during this period.

2.2. Water classification and lake mapping

The widely used methods for water classification from Landsat images include full visual interpretation and automated water extraction. Automated water detection shows high efficiency and good performance for large-scale water mapping, which can be performed by thematic classification, linear unmixing model, single-band threshold, and the spectral water index method (Feyisa et al., 2014; Fisher et al., 2016; Ji et al., 2009; Xu, 2006). The normalized difference water index (NDWI) (McFeeters, 1996) is the most popular method of automated water delineation; it separates water from non-water features based on band ratio as Eq. (1):

$$NDWI = (\rho_{green} - \rho_{NIR})/(\rho_{green} + \rho_{NIR}) \quad (1)$$

where ρ_{green} and ρ_{NIR} are the surface reflectance or top-of-atmosphere (TOA) reflectance of the green and NIR bands (Ji et al., 2009). The multi-band digital number (DN) imagery is converted into TOA reflectance by radiometric calibration (Fig. 4), which is often used in the calculation of NDWI (Li et al., 2013; McFeeters, 2013).

The optimal threshold in separating water and non-water features from NDWI imagery is the key to accurate water classification (Ji et al., 2009; Li and Sheng, 2012). It is inappropriate to use a static threshold to distinguish water with non-water covers across the whole China. First, an initial threshold of 0 was used for global-segmentation. The water and non-water components can be preliminarily separated. A buffer zone was then created for each water body unit. An optimal threshold was further determined for each water body in local-segmentation by the Otsu method (Otsu, 1979), which is a nonparametric and unsupervised method for automatic threshold selection. The Otsu method maximizes the difference between a water body and non-water features and minimizes the probability of misclassification. Water boundaries were finally extracted using the optimized threshold. This step produces a water body map, but it is still far from the accurate lake water extent mapping that is required (Fig. S1).

Shadows from mountain could result in misclassification of water body with non-water components as the similarity in reflectance patterns. This is especially important in high-mountain regions such as TP and Tien Shan. The pixels with slope threshold ($> 20°$) (M. Feng et al., 2016) and shaded relief (< 0.25) (Li and Sheng, 2012) derived from SRTM DEM (30 m, accessed at https://search.earthdata.nasa.gov) were identified as mountain shadow. The shaded relief was calculated according to the sun elevation and the azimuth angle at acquisition time of Landsat image (Wood, 1996). We downloaded the SRTM DEM

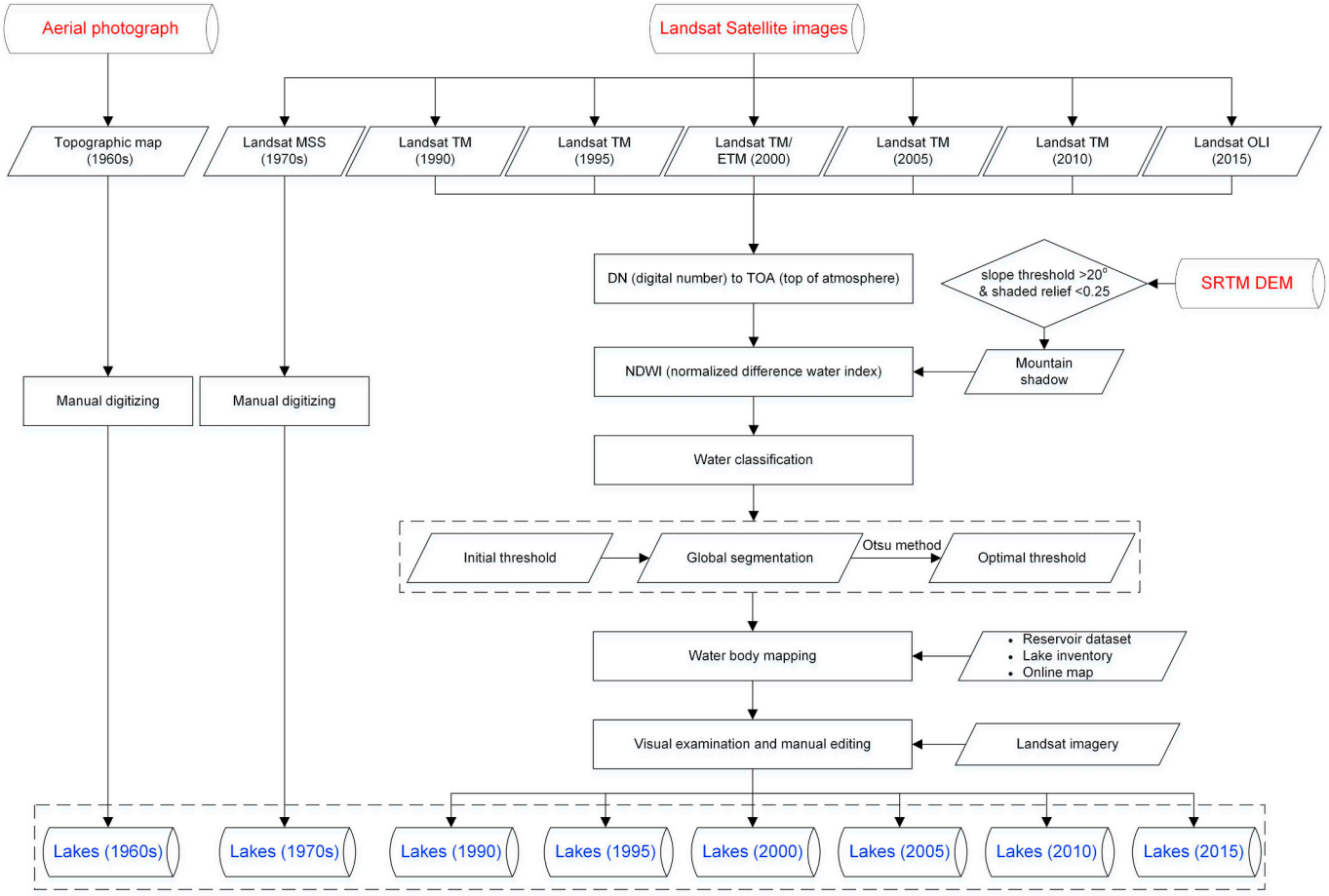

Fig. 4. Flowchart showing data used, water classification and lake mapping in China from the 1960s to 2015.

covering the entire China and merged them together. Landsat path/row boundaries (WRS-1 and -2 Shapefiles) were used to limit the extent of SRTM DEM executed. The pixels identified as mountain shadow were removed from NDWI images.

A visual inspection is still necessary after automated water extraction for lake mapping. A total of 13,890 reservoirs across China (Fig. S2) were identified to exclude them from water body data sets. In addition, the Chinese lake inventory of 2005 (Ma et al., 2010), online maps such as Baidu Map (http://map.baidu.com), and MAP WORLD (http://www.tianditu.com), and the original Landsat imagery (false color composite of bands 5, 4, 3 or 7, 4, 2) were loaded into ArcMap to conduct visual examination and manual editing of lake outlines. The manual intervention for each lake is critical to ensure a consistent output of lake boundary, although it is time consuming and labor intensive. For instance, water body mapping initially produced a number of > 20,000 units and a total area of 160,000 km^2 in 2015 (Fig. S1). After editing, including the removal of overlapped water bodies, reservoirs and rivers, the final lake data set included 2407 lakes (> 1 km^2), which have a total lake surface area of 74,395 km^2.

Lake boundaries in the 1970s were digitized manually because of the low quality of the Landsat MSS imagery at that time. Lakes in the 1960s (30 m resolution) derived from digitalized topographic map of aerial photography (1:100,000) were collected from early lake data sets (Wan et al., 2016; Wang and Dou, 1998).

3. Lake area changes tracing

We compared the difference of total lake area changes for different geographical regions and entire China between the 1960s and 2015. Moreover, a linear regression method was applied to estimate the trends of multi-decadal lake measurements. An increasing lake occurs when there is an obvious positive trend in lake area in the eight periods of 1960s–2015; and vice versa for a decreasing lake (Fig. 5). A non-parametric Mann-Kendall trend test was used to confirm the statistical confidence or significance level by the linear regression results. A non-parametric analysis of variance (ANOVA) Friedman test for paired comparison (Salerno et al., 2016) was also used to detect the statistical significance of lake area changes.

We further identified new lakes and disappeared lakes. A new lake is defined in this study as a lake that was not found in three previous continuous periods from the 1960s through 1990, but is present throughout the period 2005–2015 (Fig. 5). A disappeared lake is defined as one that existed in any of the periods in 1960s–2000, but did not appear in the last three continuous periods of 2005–2015. The original Landsat images were examined again to determine new/disappeared lakes. These strict rules were used to decide lake changes and dynamics, which is an advantage for multi-decadal lake observations in this study compared with previous studies using one period lake mapping (Ma et al., 2010; Yang and Lu, 2014).

3.1. GRACE-derived terrestrial water storage (TWS)

The NASA/DLR Gravity Recovery and Climate Experiment (GRACE) twin-satellite mission was launched in 2002. Since then, data collected by GRACE have been producing decadal and longer measurements of terrestrial water storage (TWS) anomaly, which is a composite of surface water (soil moisture, lakes, rivers, snow and glaciers), and groundwater storages at monthly sampling and with a spatial resolution

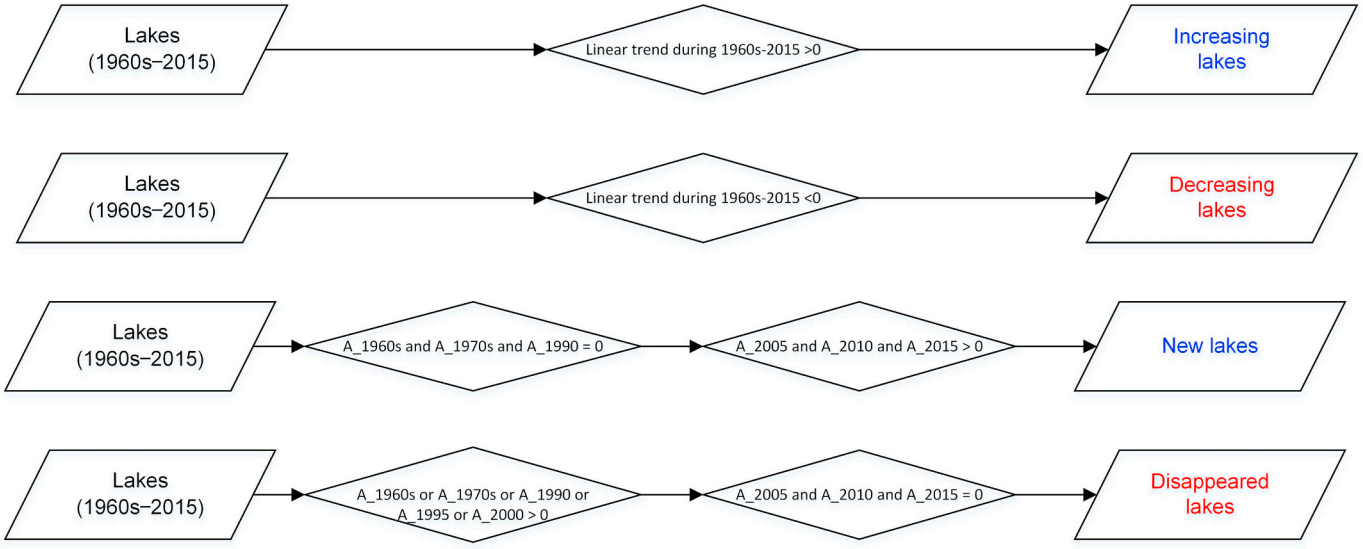

Fig. 5. The rules for deciding the newly appeared lakes, disappeared lakes, increasing lakes and decreasing lakes. A_1960s denotes the lake area in 1960s.

longer than approximately 300 km (half-wavelength). The University of Texas Center for Space Research (CSR) GRACE Level 2 Release 05 (CSRRL05) data product, spanning from January 2003 to December 2015, http://www.csr.utexas.edu/grace, was used in this study. A multi-basin inversion method was adopted to estimate TWS changes from GRACE data over the study region.

3.2. Driving factors of lake area change from climate and human activities

We used the annual temperature and precipitation observations from the China Meteorological Administration (CMA) (http://data.cma.cn) stations across China. During the period 1961–2015, continuous observations were available at 530 CMA stations (Fig. S3). The network of CMA stations in the TP is sparse, especially in the endorheic basin (only four stations), but 70% of the Plateau's lakes, in terms of both number and area are found there (Zhang et al., 2017b). A previous study compared the precipitation estimates from the Global Precipitation Climatology Project (GPCP), Global Precipitation Climatology Centre (GPCC) and PERSIANN-CDR, and found that GPCC has a relatively better performance for long-term trend analysis in the inner TP (Yang et al., 2018). The Climate Research Unit (CRU) data are inappropriate for use in the TP because they are produced through interpolation of weather station data, which is lacking due to limited stations in western Tibet. We therefore also used the monthly gridded GPCC data (V7) with a spatial resolution of 0.5° × 0.5° (Schneider et al., 2014) (ftp://ftp.cdc.noaa.gov).

The mixed effects of climate variability and anthropogenic forcing on lake area change complicate the quantification of different drivers. We used the Gross Domestic Product (GDP) index (http://www.stats.gov.cn) to represent the direct human factors, and collected the GDP of each province for the period concurrent with the lake and climate data. In addition, the satellite-recorded nighttime light data between 1992 and 2010 (https://www.ngdc.noaa.gov/eog/dmsp) were used to analyze human influences. The water levels for several lakes in the Yangtze River basin were used to show the continuous time series of lake change.

A linear regression method was used to estimate trends of temperature and precipitation and GDP changes in each sub-region and the whole of China. In addition, we employed a multiple general linear model (GLM) (Ray et al., 2015; Tao et al., 2015; Tong et al., 2017) to quantitatively evaluate the respective contributions of climatic (precipitation and temperature) and human (GDP) factors contributed to lake area change for these six regions during 1960s–2015. All data were normalized by z-score standardization before regression. There are total eight possible combinations of the variables. A backward stepwise method based on AIC (Akaike Information Criterion) was applied to select the best combination. The model with the lowest AIC was selected (Tao et al., 2015). Analysis of Variance (ANOVA) was again implemented. Finally, the quantitative contributions were obtained according to mean squares (MS).

3.3. Uncertainties of lake area measurement and attribution analysis

Uncertainties in lake area change are attributable to the following three factors:

1) Various data sources used and data with different spatial resolution. Lake areas in 1960s were derived from digitalized topographic data, which was referenced to the 1954 Beijing coordinate system with 6-degree Gauss-Kruger projection. The geo-rectified topographic maps were transformed into the Albers Equivalent Conical Projection (Ma et al., 2011). The lake boundary extracted from topographic map has a small offset relative to Landsat imagery (Ma et al., 2011). However, this has little effect on lake area estimation. In addition, the historical lake dataset in 1960s and Landsat TM/ETM+/OLI images have a spatial resolution of 30 m, but Landsat MSS has a resolution of ~60 m. The uncertainty of lake area from different spatial resolution data had been estimated at ± 0.5 pixels inside/outside the delineated lake boundary (Fujita et al., 2009; Salerno et al., 2012; Wang et al., 2013);
2) The methodologies used for water classification. We used a consistent method of automated water classification, combining with visual identification to distinguish lakes from other water components (Fig. 4). In addition, we conducted interactive post-classification comparison, and editing if the classification errors were found;
3) Intra-annual variability. We carefully selected Landsat data in the optimal period for six different geographical regions across China to minimize the uncertainty from intra-annual variations. Some images in winter were still included because of high cloud-cover such as in southeastern TP (Fig. 3). Fortunately, there are a small number of lakes in these regions. It is difficult or may be impossible to ensure all images used at the same month for each geographic region, even spanning at a 5-year interval. The multi-decadal trend regression

Table 1
Lake number and area in China between the 1960s and 2015.

Date	Lake number (≥1 km²)	Area (≥1 km²)	Lake number and area in area division (km²)											
			> 1000		500–1000		100–500		50–100		10–50		1–10	
1960s	2127	68,537 ± 130	12	20,262 ± 58	14	9287 ± 18	97	19,863 ± 23	91	6353 ± 11	347	7888 ± 13	1566	4884 ± 8
1970s	2165	66,272 ± 170	10	18,853 ± 125	14	9548 ± 85	92	19,496 ± 53	87	6191 ± 22	310	7282 ± 24	1652	4901 ± 16
1990	2149	67,815 ± 212	9	18,523 ± 106	16	11,109 ± 24	90	19,428 ± 69	41	6206 ± 15	330	7632 ± 17	1616	4917 ± 10
1995	2249	68,183 ± 211	9	18,169 ± 108	14	9949 ± 20	98	21,098 ± 39	81	5504 ± 17	375	8251 ± 16	1672	5210 ± 10
2000	2232	71,124 ± 224	10	21,267 ± 108	15	10,431 ± 31	93	19,598 ± 38	88	6238 ± 17	380	8446 ± 19	1646	5144 ± 11
2005	2415	74,053 ± 247	9	19,958 ± 116	17	12,646 ± 43	98	20,144 ± 37	93	6593 ± 18	407	9321 ± 21	1791	5392 ± 12
2010	2313	74,187 ± 244	11	21,098 ± 114	16	10,780 ± 45	104	21,650 ± 39	93	6463 ± 15	386	8919 ± 19	1703	5277 ± 12
2015	2554	74,395 ± 247	10	19,785 ± 110	15	10,758 ± 58	110	22,534 ± 34	95	6562 ± 15	394	8992 ± 19	1930	5765 ± 11

analysis used in this study can decrease errors in the imagery which may have caused false signals of intra-annual variability of lake area changes, and more appropriately capture inter-annual variation, especially at a significant level ($P < 0.1$).

The multiple GLM analysis is used to quantify the relative contribution of climate and anthropogenic factors. The drivers of lake changes in different regions across China could be different and complicated. To maintain the consistency of data in different regions and coincident period with lake area observations, we used the GDP data to evaluate the effect of human activities. It has the advantage of integrating multiple socio-economic factors even though the detailed components are not enumerated here.

4. Results

4.1. Multi-temporal lake changes

Total lake area in whole China increased by 9% from 68,537.15 ± 67.01 km² in 1960s to 74,395.21 ± 131.76 km² in 2015, with a significant difference based on the Friedman test ($P < 0.01$) (Tables 1–2). Changes in lakes area present sharp differences between the 1960s and 2015, with a positive rate of 34% for increased lakes and negative rate of −25% for decreased ones. The linear trend of lake area change during 1960s–2015 shows a water surface area gain of 138.91 ± 40.80 km² yr^{-1} (Fig. 6 and Table 3). Total lake number (lakes with size ≥ 1 km²) has increased by 20% from 2127 in 1960s to 2554 in 2015. Respectively, expanding lakes have increased by 836 (88%) from 945 in the 1960s to 1781 in 2015, but shrinking lakes have decreased by 409 (35%) from 1182 in the 1960s to 773 in 2015 (Table 2).

The geographically heterogeneous variations in lake number and area are clear (Fig. 6 and Tables 2–3). TP, XJ, and NE respectively exhibit a large lake area expansion of 15%, 27% and 37%, respectively, excluding YG which has a slight increase of 0.2% between the 1960s and 2015. MP and EP display a lake area shrinkage of 22% and 7%, respectively. Lake number (size ≥ 1 km²) in TP, XJ, and NE has an abundant increase of ~150. However, the number of lakes (size ≥ 1 km²) in EP has decreased by 49. The trends of lake area change during 1960s–2015 reveal apparent increases of 103.00 ± 42.49, 25.47 ± 6.39, and 22.42 ± 9.02 km² yr^{-1} for TP, XJ, NE, respectively. MP revealed a water loss of 21.97 ± 10.78 km² yr^{-1}. EP and YG did not show a significant trend of lake area gain or loss.

4.2. Spatial patterns of lake distribution and evolution

Large lakes (size > 1000 km²) are mainly distributed in TP and EP (Fig. 7). Most lake changes are also mainly located within two specific regions of China (Fig. S4). Spatial patterns of lake area change show that expanding lakes and rapidly growing lakes (Fig. 8) are mainly found in TP and NE (80%). MP, EP and YG together have 69% of the decreasing lakes in their areas. The shrinking lakes in the TP are mainly located along the southern border, and the number of lakes and their areas are small relative to those for the increasing lakes.

Lakes size analysis reveals different patterns of evolution (Fig. 9). The size of the expanding lakes in NE, and EP is small (< 50 km²), and the magnitude of increase is slow. Lakes in the TP have larger sizes and have increased rapidly, especially in the central-northern plateau. There, the dominant small lakes (< 10 km²) show a shrinking trend. Large shrinking lakes are mainly distributed in eastern MP, along the lower reaches of the Yangtze River in EP and southern TP. Lake number and area changes in 2015 relative to the 1960s are grouped according to area divisions, which can decrease the area variability of small lakes (Fig. 10). The numbers and areas in TP, XJ and NE have increased sharply, but MP and EP clearly show an opposite pattern.

4.3. Lake dynamics of appearance and disappearance

The appearance of new lakes and the disappearance of lakes between 1960s and 2015 are quantified here (Fig. 8). We find that 141 lakes have emerged and 333 lakes have vanished. The new lakes are predominately distributed in TP, XJ and NE (94%), with a particularly large lake area (40–60 km²) appearing in XJ. The disappeared lakes are mainly situated in MP, NE close to MP and EP (83%). The vanishing lakes in EP are widespread (Fig. 11) with the lake boundaries diminishing due to rapid urbanization. Thus, it is evident that urbanization has resulted in the shrinking or vanishing of the lakes in the EP region.

4.4. Lake changes related with TWS

GRACE-derived TWS changes between 2003 and 2015 in the TP match well with lake (surface) area variations derived from Landsat data (Fig. 12). This is ascribed to the increased mass in Inner TP being dominated by lake storage increase during the recent decade and a half (Zhang et al., 2013, 2017c). The TWS change in XJ showed a significant decrease, but precipitation has increased (Fig. 13), which could be due to the intensified human activity of groundwater withdrawal (Deng and Chen, 2017). The TWS in MP indicated a slight decrease between 2003 and 2014 and subsequent recovery in 2015, which is consistent with precipitation variations (Zhang et al., 2017b). Both the TWS and lake changes in NE are coincident with an increasing trend. The number and area of lakes in YG are small and disproportionate to compare with GRACE TWS anomaly (Table 2 and Fig. S5).

5. Discussion

5.1. Comparison of our lake inventory with previous studies

The previous studies from (Ma et al., 2010; Yang and Lu, 2014) mapped China's lakes in ~2005. (Pekel et al., 2016) produced a global

Table 2
Changes in lake number and area in 2015 relative to the 1960s in each sub-region and whole China. A non-parametric analysis of variance (ANOVA) Friedman test for paired comparison (Salerno et al., 2016) is used to detect the statistical significance of lake area changes between the 1960s and 2015.

	Zone	Lakes increased				Lakes decreased				Total			
		1960s	2015	Change	Change (%)	1960s	2015	Change	Change (%)	1960s	2015	Change	Change (%)
Lake area (km^2)	TP	29,291.7-7 ± 20.68	36,522.0-2 ± 36.28	7230.2-5 ± 41.76	25**	7552.8-0 ± 12.91	5999.3-0 ± 15.66	−1553.5-0 ± 20.30	−21**	36,844.5-8 ± 24.38	42,521.3-3 ± 39.52	5676.7-5 ± 46.43	15**
	XJ	3120.6-1 ± 5.06	5128.9-1 ± 11.85	2008.3-0 ± 12.89	64**	2141.8-3 ± 6.99	1550.6-8 ± 6.86	−591.1-5 ± 9.79	−28**	5262.4-4 ± 8.63	6679.5-9 ± 13.69	1417.1-5 ± 16.18	27**
	MP	964.59 ± -2.69	1462.7-6 ± 5.72	498.16 ± -6.32	52**	4640.7-5 ± 9.72	2919.0-5 ± 8.85	−1721.7-0 ± 13.15	−37**	5607.4-1 ± 10.08	4383.6-5 ± 10.55	−1223.7-6 ± 14.560	−22**
	NE	1251.4-8 ± 6.71	2748.3-4 ± 16.74	1496.8-6 ± 18.03	120**	1802.9-0 ± 3.43	1440.9-1 ± 4.75	−361.9-9 ± 5.86	−20**	3054.3-8 ± 7.53	4189.2-5 ± 17.39	1134.8-7 ± 18.95	37**
	EP	4187.7-9 ± 47.05	6154.5-8 ± 108.92	1966.7-9 ± 118.6-5	47**	12,375.8-0 ± 37.68	9259.9-9 ± 57.26	−3115.8-1 ± 68.54	−25**	16,561.5-2 ± 60.27	15,412.7-3 ± 123.05	−1148.7-9 ± 137.02	−7**
	YG	250.30 ± -1.38	347.85 ± -2.55	97.56 ± 2-.89	39**	956.53 ± -5.27	860.81 ± -7.13	−95.7-1 ± 8.87	−10**	1206.8-2 ± 5.45	1208.7-3 ± 7.57	1.84 ± 9.3	0.2
	Whole China	39,066.5-5 ± 52.16	52,364.-5 ± 116.8	13,297.9-1 ± 127.9-1	34**	29,470.0-6 ± 42.07	22,030.7-5 ± 61.02	−7439.8-5 ± 74.11	−25**	68,537.1-5 ± 67.01	74,395.2-1 ± 131.76	5858.0-6 ± 147.3	9**
Lake number	TP	581	802	221	38	319	245	−74	−23	900	1047	147	16
	XJ	50	224	174	348	46	26	−20	−43	96	250	154	160
	MP	95	207	112	118	229	127	−102	−45	324	334	10	3
	NE	109	324	215	197	128	64	−64	−50	237	388	151	64
	EP	93	181	88	95	425	288	−137	−32	518	469	−49	−9
	YG	17	43	26	153	35	23	−12	−34	52	66	14	27
	Whole China	945	1781	836	88	1182	773	−409	−35	2127	2554	427	20

** $P < 0.01$.

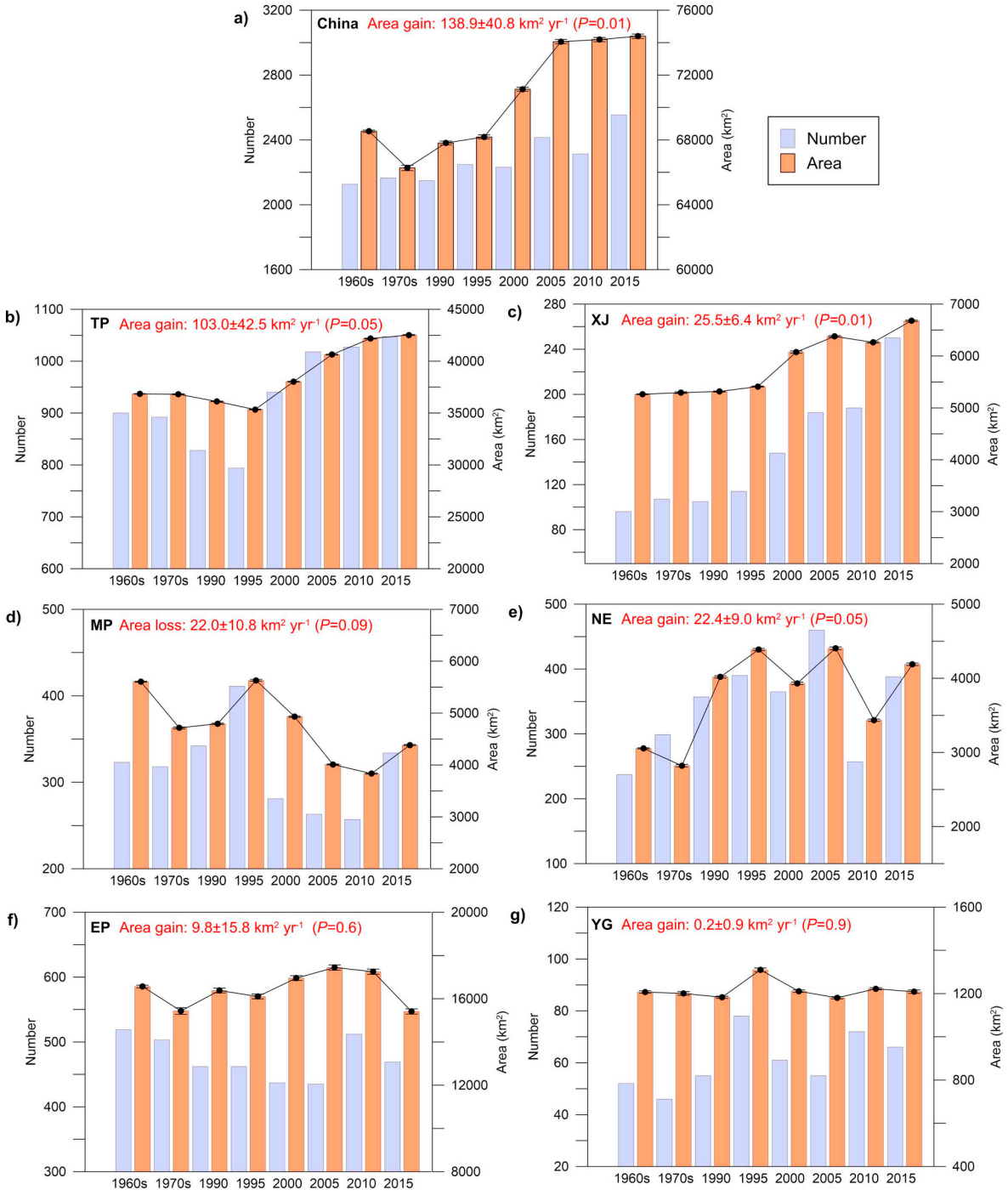

Fig. 6. Decadal variations of total number and area of lakes > 1 km^2 from 1960s to 2015. a) Whole China. b) TP. c) XJ. d) MP. e) NE. f) EP. g) YG. Linear trends of lake area change and significance level are labelled. Error bars indicate the uncertainty of lake area mapped from remote sensing data.

surface water product, which is different from lake mapping. We compared the regional differences in lake number and area in ~2005 between our lake inventory and previous studies (Ma et al., 2010; Yang and Lu, 2014) and analyzed the possible reasons (Fig. 14, Table S1). These discrepancies could be mainly attributed to: 1) the area variability of small lakes (1–2 km^2) or salt lakes; 2) area calculated for transboundary lakes such as Xingkai Lake; 3) seasonal variability for lakes in the Yangtze River basin.

We also summarized the advantage of our data sets (Table S1). Inventories of lakes (size ≥ 1 km^2) are first drawn up by surveys from the 1960s through 2015 over eight stages. The updated lake inventory is particularly important because the recent decade is the time during which climate change impacts are likely to be the greatest as well as when there have been more rapid increases in economic development and urbanization. The long time-series lake area is used to detect the characteristics of lake evolution, which is better than the differences of lake area between two-period data. A high classification accuracy of lake is reached by a strict quality control in data and methods used. The uncertainty of lake area mapped could be small relative to the dramatic changes of lake area during the past ~55 years in China.

Table 3
Changes in lake area, temperature and precipitation from CMA stations, and GDP in each sub-region and the whole of China.

Region number	Region name	Lake change ($km^2\ yr^{-1}$)	Temperature change ($°C\ yr^{-1}$)	Precipitation change ($mm\ yr^{-1}$)	GDP change (billion yr^{-1})
1	TP	103.00 ± 42.49*	0.03 ± 0.003**	0.77 ± 0.19**	4.08 ± 0.50**
2	XJ	25.47 ± 6.39**	0.03 ± 0.004**	0.87 ± 0.18**	11.98 ± 1.37**
3	MP	−21.97 ± 10.78	−0.03 ± 0.004**	−0.42 ± 0.40	75.65 ± 9.29**
4	NE	22.42 ± 9.02*	−0.03 ± 0.005**	−0.09 ± 0.64	79.05 ± 8.66**
5	EP	9.82 ± 15.80	0.02 ± 0.003**	0.79 ± 0.88	670.32 ± 76.09**
6	YG	0.17 ± 0.86	0.02 ± 0.003**	−1.19 ± 0.48*	83.02 ± 9.97**
All	Whole China	138.91 ± 40.80*	0.03 ± 0.003**	0.12 ± 0.27	924.09 ± 105.79**

** $P < 0.01$.
* $P < 0.05$.

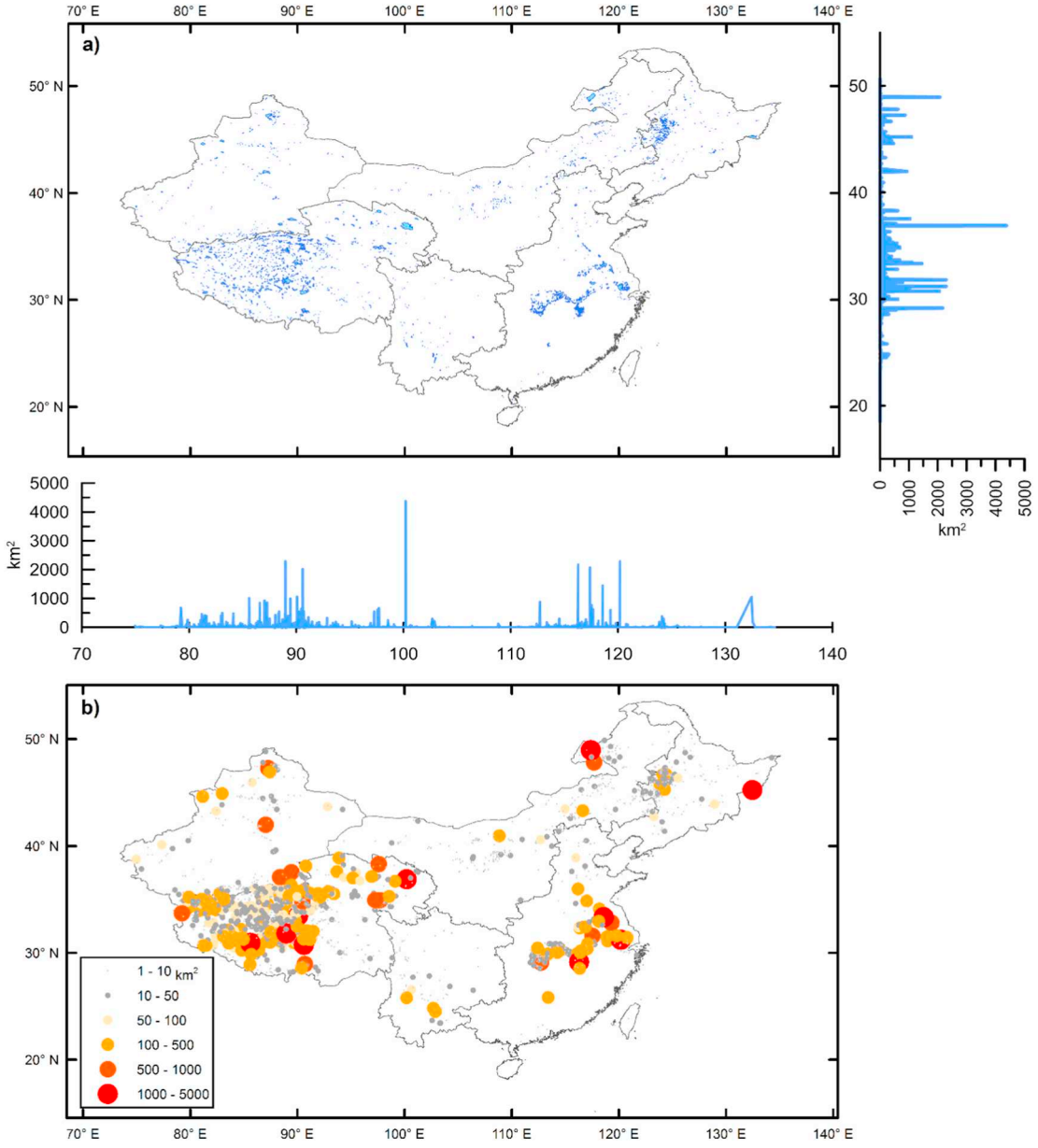

Fig. 7. Lake mapping using the data in 2015. a) Lake mapping, and histograms based on longitude (below) and latitude (right). b) Lake distribution based on lake sizes.

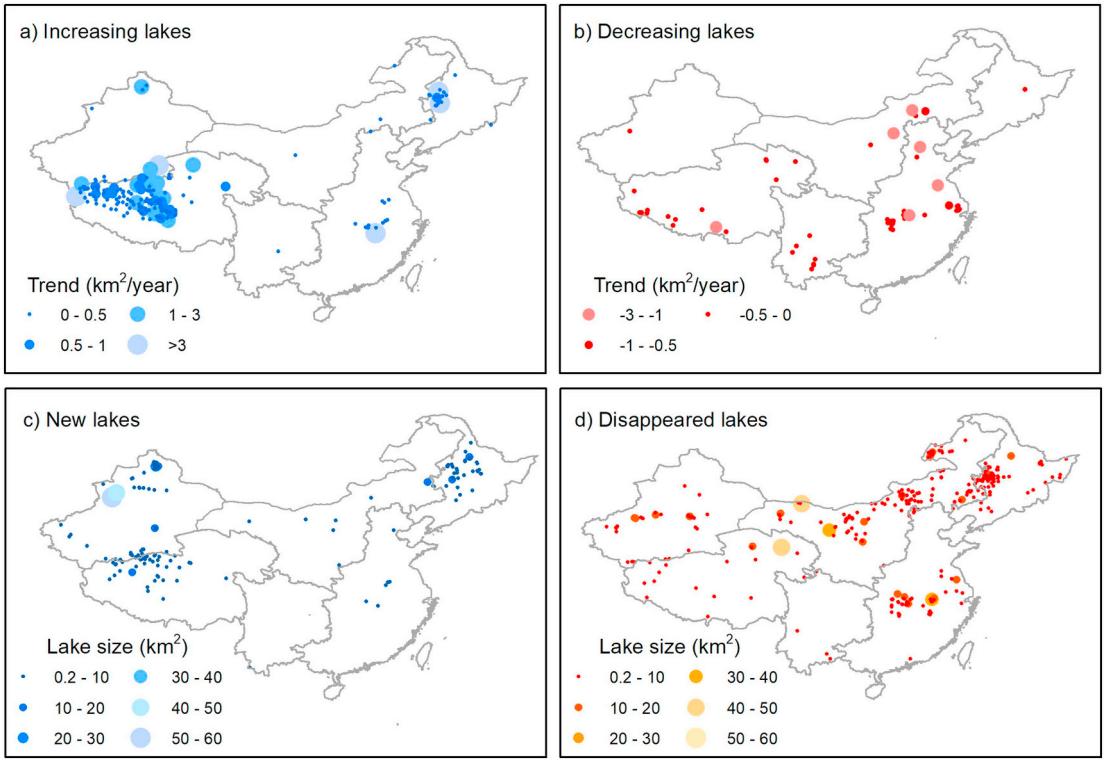

Fig. 8. Lake changes from the 1960s through 2015 in China. a) Increasing lakes (positive linear trends between the 1960s and 2015). b) Decreasing lakes (negative linear trends between the 1960s and 2015). Only lakes with linear trends with $P < 0.1$ are shown. In addition, lakes < 5 km^2 and rates of lake area change smaller than 0.02 $km^2\ yr^{-1}$ are also omitted as is the variability of small lakes and lakes with little area changes. All lakes with increasing or decreasing trends are shown in the Supporting Information. c) Newly appeared lakes. d) Disappeared lakes.

The comparisons of classification accuracy of our data present good performance with these previous data sets (Ma et al., 2010; Yang and Lu, 2014). First, we select Landsat data for different geographic regions in same optimal month to decrease intra-annual variations. Although 5-year interval Landsat data is selected, it is still inescapable some data outside the optimal season are selected such as southeastern TP. Fortunately, these regions have a small coverage of lake distribution. This will not result in large uncertainties of lake number and trend analysis. Second, mountain shadow derived from 30-m SRTM DEM is used to reduce the misclassification of water body because of topography effects. Additionally, the global-local segmentations with optimal thresholds determined from the Otsu method are employed to distinguish water from non-water features. This method shows high accuracy and efficiency in extracting waterbody boundary. Moreover, visually inspections combining with original Landsat images are performed. Finally, a comprehensive reservoir data set, wetlands and rivers are used to remove from non-lake water bodies, combining with visual examination again. All these steps ensure a high-quality water classification and lake mapping.

It is important that uniform criteria should be adopted throughout data processing. The operator should work patiently and carefully in data selecting and water body classification. It could be better for the same operator to work in classification and examination for same region. Cross-checking from different operators is necessary for final output of lake data set.

5.2. Effects of climate and human activities on lake changes

The geographically heterogeneous changes in lake number and areas are driven by complex processes of climate change and direct human activities (Ma et al., 2010; Tao et al., 2015; Yang and Lu, 2014). The temperature in all the study regions in China has been increasing with the fastest warming rate of 0.03 ± 0.003 °C yr^{-1} ($P < 0.01$) in the TP (Fig. 13 and Table 3) (Duan and Xiao, 2015; Shi et al., 2014). Northwestern, northeastern and southeastern China are getting wetter and central China is getting drier. Human activities have been intensifying, particularly in eastern China with its relatively fast economic development and industrialization (Xu et al., 2016). The relative contributions of climate and human effects on lake area changes were evaluated from GLM analysis (Table S2).

Increasing of lake areas in the TP appears to be driven by multiple sources of water supply including net precipitation onto the lake surface and precipitation-induced runoff from upstream catchments, snow and glacier melting, and permafrost degradation (Song et al., 2014; Zhang et al., 2017c; Zhou et al., 2015). Precipitation has shown an increasing trend of 0.77 ± 0.19 mm yr^{-1} ($P < 0.01$, Fig. 13 and Table 3), with a dominant contribution (Table S2). However, quantifying the individual component is difficult because of the limited network of weather stations in the dominant lake areas. Many studies have reported that increased precipitation has contributed to the majority of lake water increase (> 70%) in the endorheic basin (Li et al., 2017; Li and Lin, 2017; Tong et al., 2016; Zhang et al., 2017c; Zhou et al., 2015). The rapid expansion of lake area since 1995 is driven by wetter climate (Figs. 13 and 15), which is attributed to enhanced water vapor transport to the north-central plateau and redistribution by the local atmospheric circulation (Gao et al., 2015; Yang et al., 2011; Zhang et al., 2017b). Topographic features (geomorphology) can affect the water vapor transmission, which can further impact the distribution and change of lakes. For example, a 'corridor-barrier' effect formed by the longitudinal range-gorge terrain has a major impact on the lake change in the Henduan Shan region in southeastern TP (X.I.N. Wang et al., 2017). Lake change driven by direct human activity in the TP can be ignored

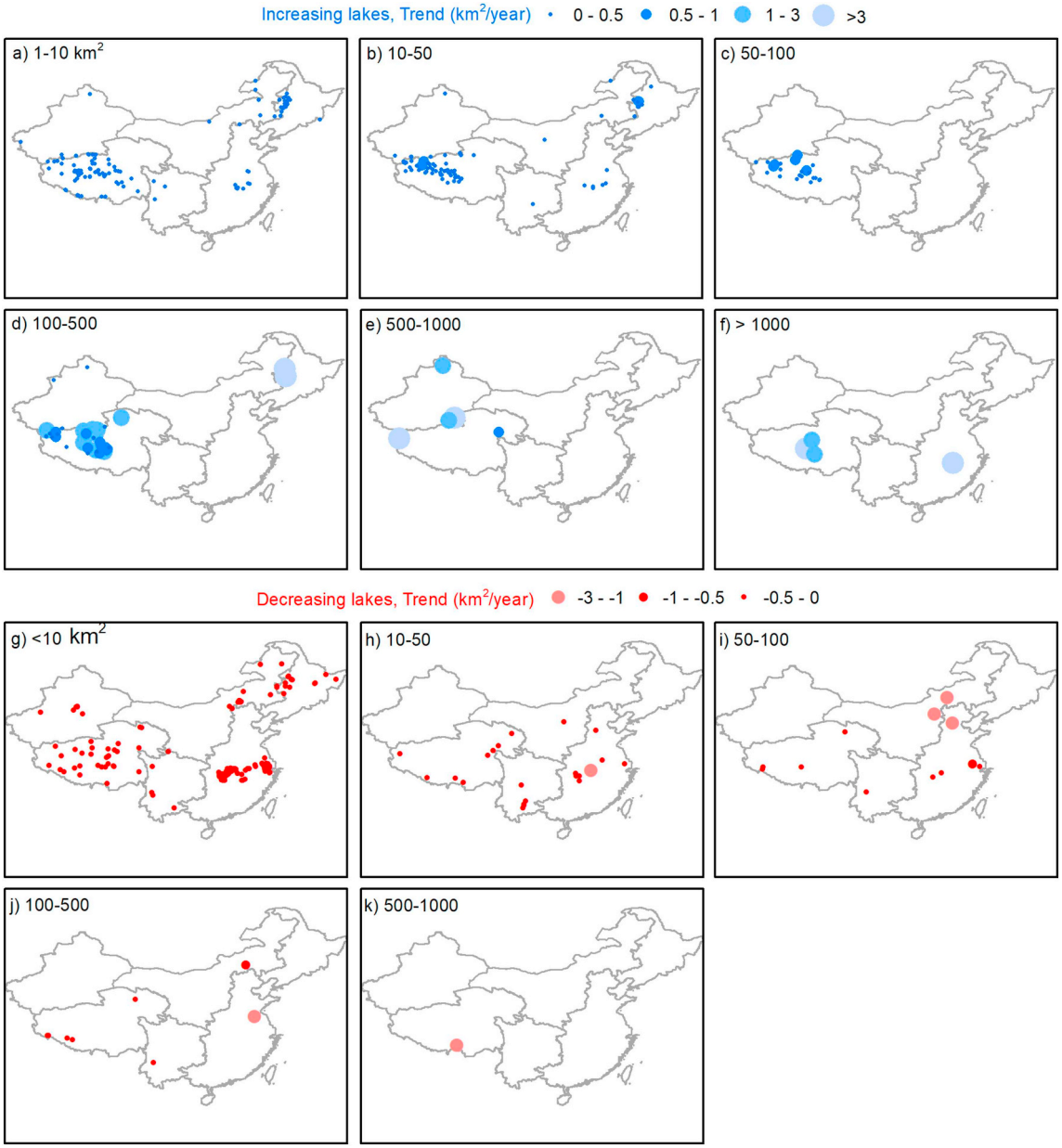

Fig. 9. Spatial pattern of lake area changes for increasing lakes or decreasing lakes in different sizes.

due primarily to sparse population in this region, especially in the endorheic basin (the Qiangtang Plateau), where most of the TP's lakes are located.

Precipitation in XJ is increasing at a rate of $0.87 \pm 0.18\,\mathrm{mm\,yr^{-1}}$ ($P < 0.01$, Table 3). The spatial variations in temperature and precipitation indicate the overall warmer and wetter climate, especially in the northern part with more lakes. The increased precipitation has been the major contributor to recent lake enlargement (Table S2). The inflection point of lake change in 1995 in XJ is consistent with the time series of precipitation change, which is also similar in the TP. The cryosphere (snow/glacier and permafrost) changes in XJ also contributed to lake storage increase. The increased precipitation in arid and semiarid XJ is due to the thermodynamic component of moisture flux convergence induced by increased specific humidity (Peng and Zhou, 2017). Direct anthropogenic influence, such as increased agricultural irrigation, has resulted in intensification of groundwater withdrawal (Deng and Chen, 2017). The inverse correlation between decreased TWS and increased precipitation since 2003 (Figs. 12–13) also suggests intensified human activities due to increased population, as evidenced by satellite thermal imagery observations indicating increased nighttime light emission across China (Dai et al., 2017; Wu et al., 2013) (Fig. S6) as well as increased water consumption (Deng and Chen, 2017).

Time series of lake changes in MP indicated an overall decrease with a slight increase in 1995. The precipitation in this region also showed a generally decreasing trend ($-0.42 \pm 0.40\,\mathrm{mm\,yr^{-1}}$, $P > 0.05$). The time-series of precipitation changes matched well with lake area changes (Zhang et al., 2017b). This study revealed that precipitation changes play a dominant role in lake area changes (Table S2). However, intensive human activities should not be ignored for lake loss in this warmer and drier region (Tao et al., 2015).

Changes in precipitation in NE revealed a generally decreasing trend although it was not significant; however, regional differences occurred. Lakes were mainly located in the northwestern corner, where precipitation was increasing (Figs. 13, 15). Climate change was the

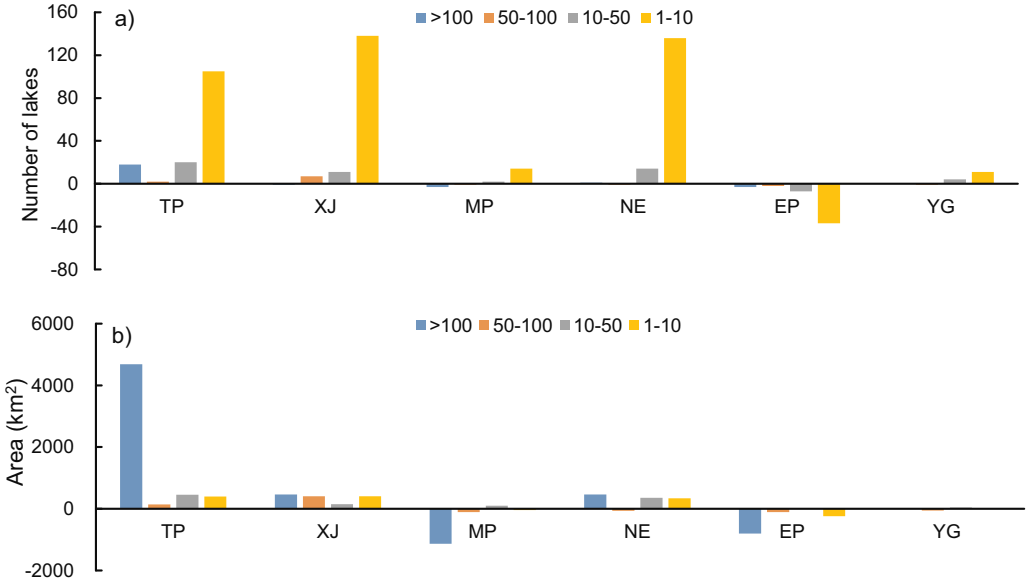

Fig. 10. Changes in lake number and area in 2015 relative to the 1960s in groupings of 1–10, 10–50, 50–100, > 100 km^2. a) Number change. b) Area change.

dominant driver of lake variations, especially from warmer temperature (Table S2), but human activities such as conversion of lake wetland to cultivated land, and construction of water conservancy projects such as reservoirs and embankments should raise concern (Li et al., 2014).

Lakes in EP (the lower reaches of the Yangtze River), which holds the largest freshwater resources in China, did not reveal a significant trend in total lake area ($P > 0.1$) (Fig. 6); although the lake numbers have decreased, and the precipitation has increased over the last five decades (Fig. 13). The strongest observed human activities have occurred in this region (Figs. 13 and S6), which contributed to 35% of the total lake shrinkage (Table S2), suggesting that urban development has resulted in lakes vanishing or lake shrinking (Ma et al., 2010). Ninety lakes have disappeared between 2000 and 2016 in Wuhan City in the middle reaches of the Yangtze River because of the anthropogenic effect of lake in-filling as part of the process of urban expansion (http://politics.caijing.com.cn/20160708/4145947.shtml). Water level of Dongting Lake (Han et al., 2016), Hongze Lake (Wen et al., 2006), Poyang Lake (R. Wang et al., 2017), Tai Lake (Wang et al., 2016) and Tianmu Lake (Huang et al., 2007) downstream of the Three Gorges Dam (TGD, the world's largest hydroelectric dam) in the Yangtze River basin have shown a decline since 2003 (Fig. S7). For example, the water level of Poyang Lake (the largest freshwater lake in China) has gone down since the operation of the dam, and this decrease is linked with the operation of the TGD (L. Feng et al., 2016). The impoundment of the dam has also caused a significant decrease in the inundated area of the Poyang Lake and the Dongting Lake (Feng et al., 2013). Intensified sand mining in the Poyang Lake has contributed to a decline in lake level since 2001 (Feng et al., 2015). In addition, illegal sand dredging has rapidly increased in Hongze Lake since 2012, which could further decrease and degrade the natural water balance and regional ecological environment, respectively (Cao et al., 2017).

The precipitation in YG presented an overall decrease, but with apparent regional variations. Lake area is rising in the regions with increased precipitation, and vice versa (Fig. S8). However, these regional differences in lake area were insignificant overall, as confirmed by the Friedman test ($P > 0.05$) (Table 2). Human activities such as land reclamation and increased water consumption by industry and agriculture have aggravated the contraction of lakes (Li et al., 2010), which accounts for a similar proportion of decrease (~35%) with EP (Table S2).

5.3. New scientific knowledge

In this study, we have developed a comprehensive lake area dataset for multi-decadal analyses. The dataset includes all lakes in China with areas ≥1 km^2, and at 5-year temporal sampling, which have not yet been achieved in China or elsewhere in the world. Pekel et al. (2016) produced a global surface water data set, but lake mapping across China need data selected at a relative stable season for different geographic regions, and manual visual inspection to separate lakes from other water components. Previous studies have mapped lake areas in China using two periods data (Ma et al., 2010; Yang and Lu, 2014), wetland change (with a different definition in lake) between 1978 and 2008 (Gong et al., 2010; Niu et al., 2012), and multi-temporal lake inventory (1960s, 2005, 2014) for the TP (Wan et al., 2016). However, these studies mapped lakes across China in ~2005, and compared it with the first Chinese lake inventory, and could not delineate trends of long-term lake observations.

Based on data sets produced in this work, we examined the regional differences of lake evolutions and dynamics across China during 1960s–2015. The intra-annual variability can induce uncertainty in examination of lake area change. For example, the water exchange between the main stream of the Yangtze River and lakes (e.g. Dongting Lake, Poyang Lake, Taihu) can cause the fluctuation of lake shoreline expansion and shrinkage. We selected the lakes at the stable months and used robust linear regression to detect their trends, which is not possible with simple two-stage lake mapping. In addition, new lakes and disappeared lakes are also determined with multi-period observations. The lake inventory produced in this study is an asset for future lake area change and simulation as a reference baseline.

Our results expand on previous works, which concluded that the differences in China's lake numbers and sizes are due to climate change in North China and human activities in South China (Ma et al., 2010). During the recent decades, lakes have appeared or disappeared and lake areas have extensively changed, and also vary significantly in different geographical regions in China, primarily because of rapid climatic and ecological change, as well as intensified human activities in some regions. The respective contributions from climate change and direct human activities were quantitatively assessed in this study. The change in precipitation has predominately driven lake changes in TP, XJ, and MP, respectively (Table S2). The change in temperature has a greater

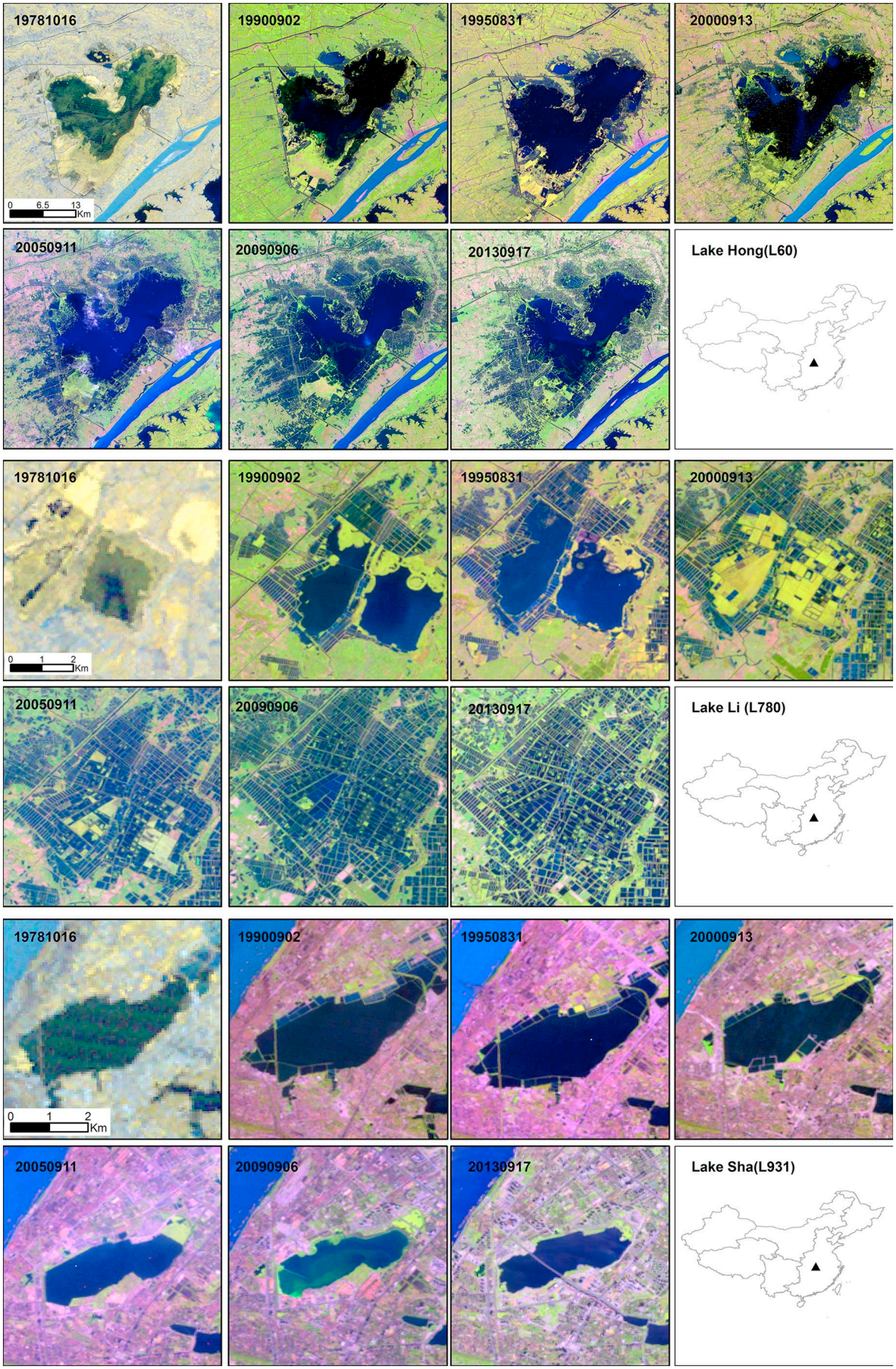

(caption on next page)

Fig. 11. Examples showing the shrinking or disappearing lakes in Eastern Plain. False color composite images (NIR, red and green bands for Landsat MSS in 1978 and NIR, SWIR 1 and red bands for Landsat TM/ETM/OLI in 1990–2013) are shown. (For interpretation of the references to color in this figure legend, the reader is referred to the web version of this article.)

contribution relative to precipitation for lakes in NE. The human activities have the most significant contributions of ~35% for lake shrinkage in EP and YG relative to other regions. Overall, climate changes such as precipitation and temperature have played a dominant role across China, however, direct human activities have also contributed noticeably to lake shrinkage in EP and YG.

In addition to the generation of this high level multi-decadal lake dataset available for the scientific community and public, this study has improved our understanding of lake dynamics and identified factors which drove lake evolutions across China. Our results could inform decision-makers and relevant stakeholders in land-use choices and water-resource planning and management, assist with mitigating lake deterioration, and improve the Chinese lake development modelling.

6. Conclusions

Lake area changes across China since the 1960s were examined using remotely sensed data. Lakes over the whole of China showed an evident area increase, especially after 1995. Geographically heterogeneous variations in lake number and lake area over the past five decades were evident. Lake areas in TP, XJ and NE have greatly extended, but have shrunk in MP. Climate changes have played the dominant role in regulating the lake changes across China. However, human activities are also responsible for lake shrinkage in EP and YG relative to other regions. We find 141 new lakes mainly in TP and XJ; these result from increased precipitation together with cryosphere contribution. We find 333 lakes have disappeared, mainly in MP, a

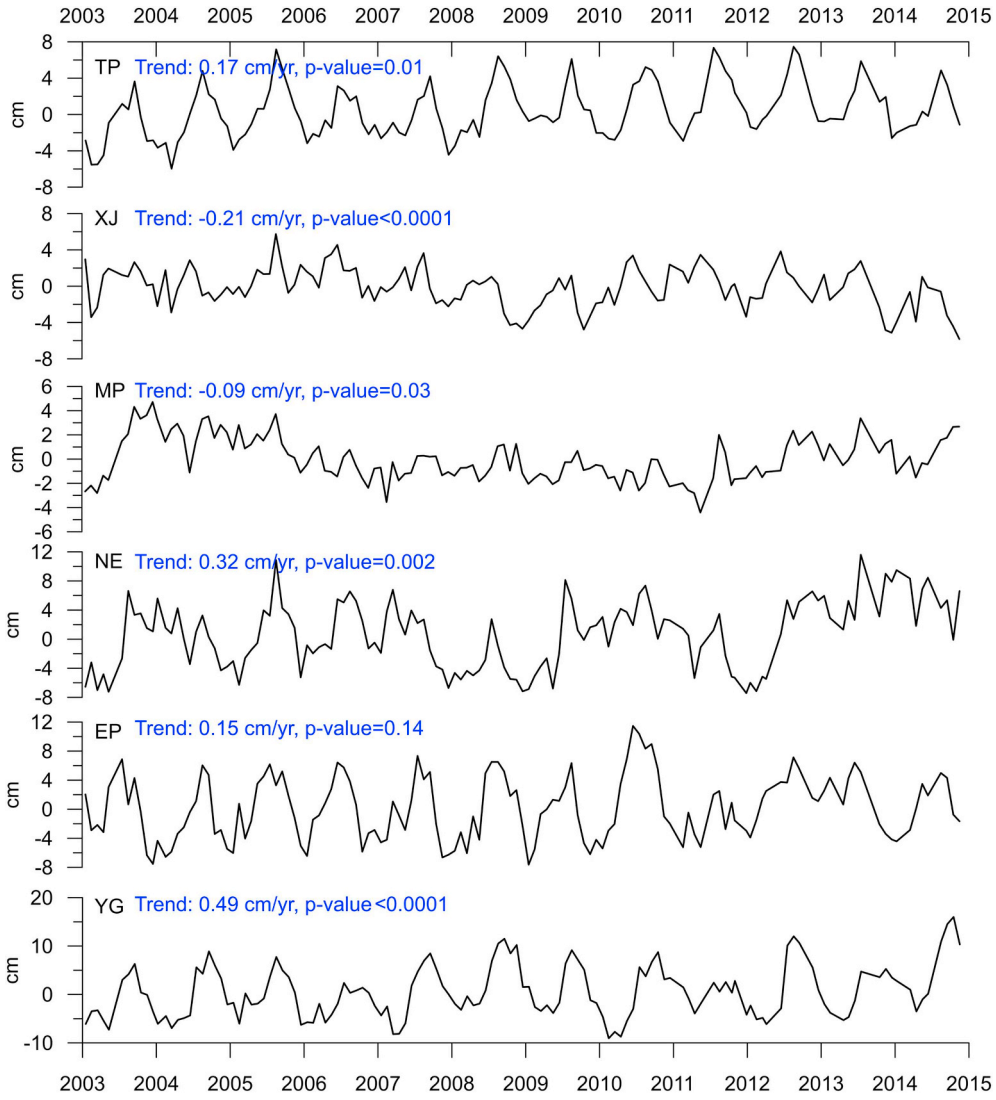

Fig. 12. Times series of the terrestrial water storage (TWS) from GRACE data in six sub-regions of China between 2003 and 2015.

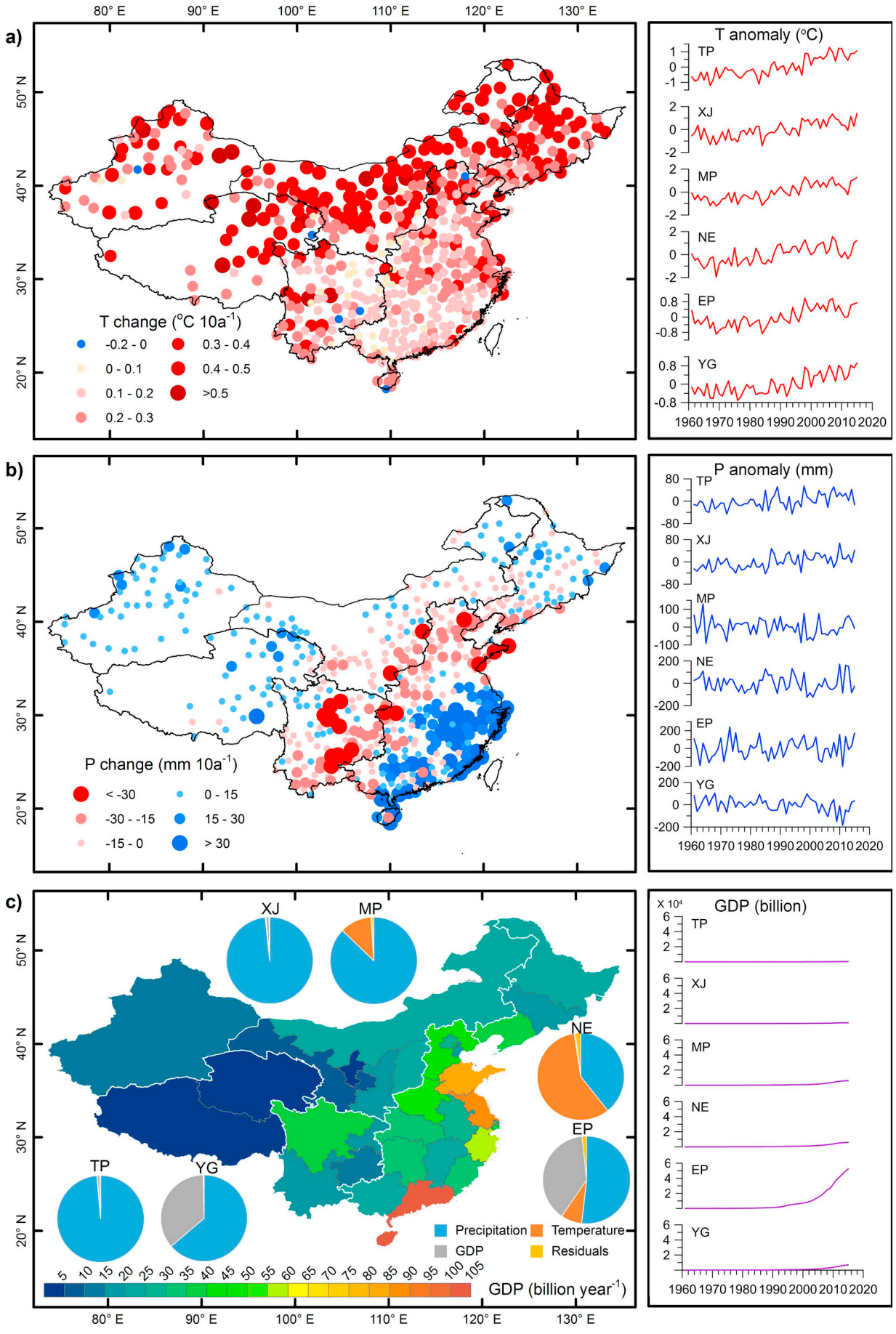

(caption on next page)

Fig. 13. Major drivers for lake changes between the 1960s and 2015. a) Changes in temperature (T) from the China Meteorological Administration (CMA) stations. b) Changes in precipitation (P) from CMA stations. c) Changes in gross domestic product (GDP). Inset shows the contributions of climate (precipitation and temperature) and human activities (GDP) for lake changes. Time series of temperature and precipitation anomaly, and GDP for each study region is shown in the right panels.

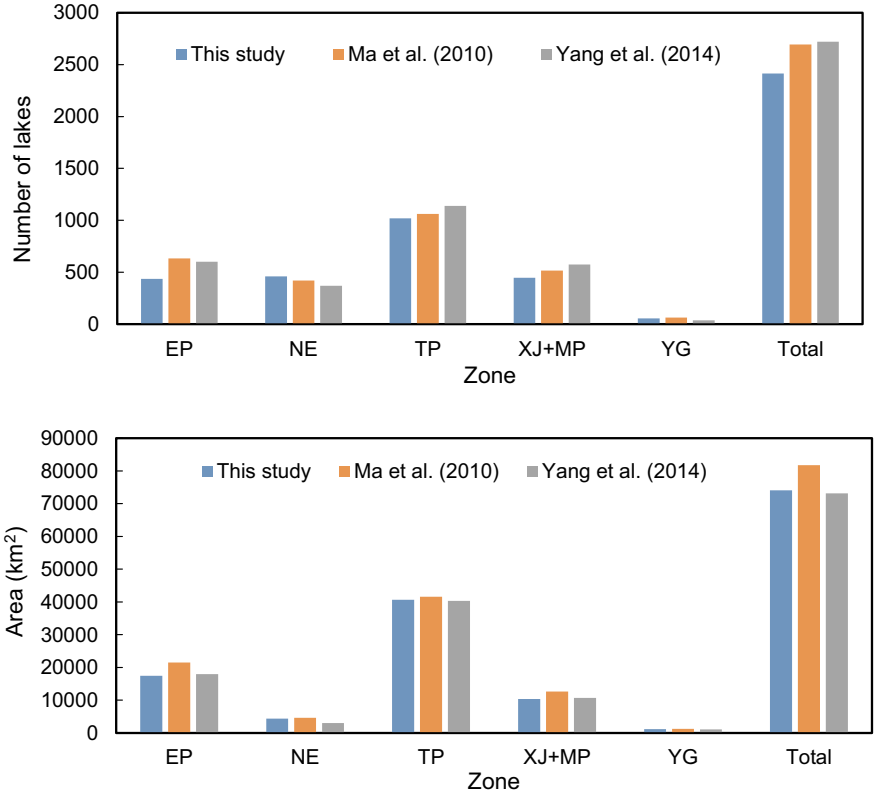

Fig. 14. Lake number and area in 2005 in this study compared with the results from Ma et al. (2010) in 2005–2006 and Yang and Lu, (2014) in 2005–2008.

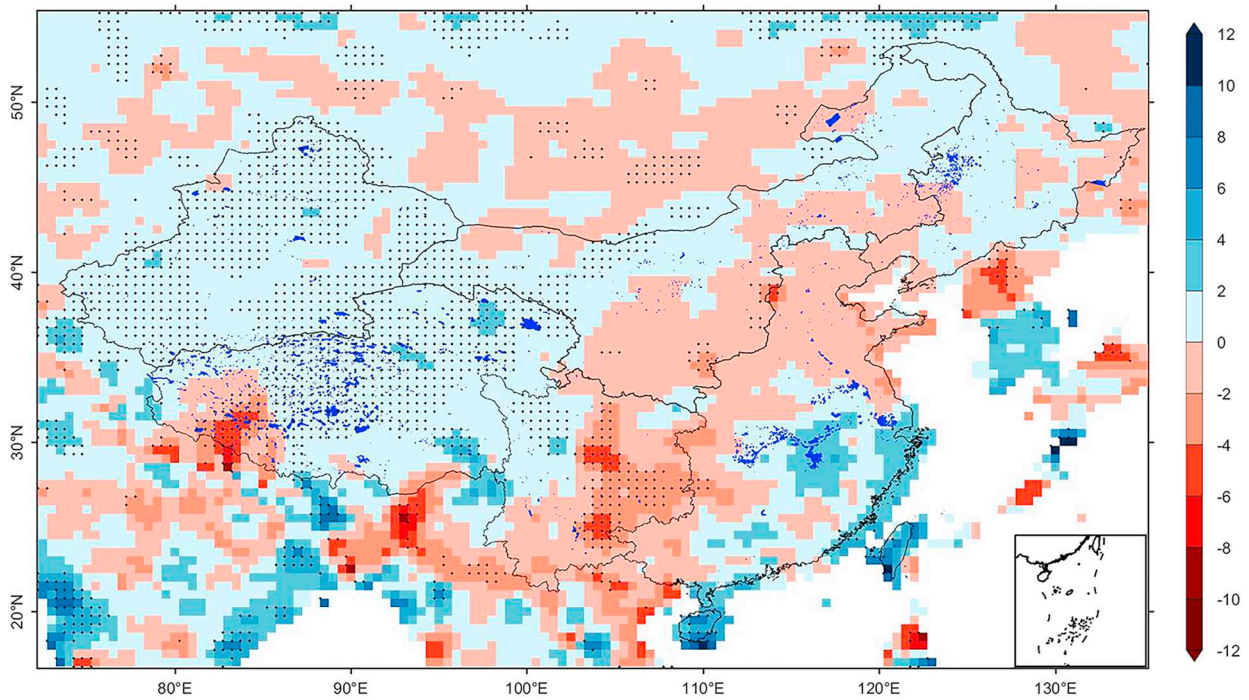

Fig. 15. Spatial patterns of linear trends of precipitation (mm yr^{-1}) from GPCC data during 1961–2013. Lake distributions are overlapped. The "+" indicates the significant linear trends at 95% confidence level.

result of warmer and drier climate, and in EP from urbanization. The intensive human activities in China, especially in eastern China with its increasingly denser population, rapid urbanization and industrialization are apparent from space observation and socio-economic data. As the population in China migrates from villages to urban areas, the number of houses in China has doubled several times in recent years. China's economy has been continuously growing, anthropogenic influence has been adversely affecting freshwater lakes, an invaluable water resources, more than at any other time in history. This new long-term lake evolution data set provides a foundation for evidence-based decision support for water resources management and environmental protections in China.

Acknowledgements

This study was supported by grants from the Natural Science Foundation of China (41871056, 41571068, 21661132003), the Strategic Priority Research Program (A) of the Chinese Academy of Sciences (XDA20060201). The Landsat imagery used in this study are from USGS EROS Data Center and NASA (https://glovis.usgs.gov). The in situ temperature and precipitation measurements were acquired from CMA (http://data.cma.cn). The NASA/DLR GRACE satellite mission data products were provided by the University of Texas at Austin, Center for Space Research (CSR) (http://www.csr.utexas.edu/grace). The NOAA DMSP-OLS data set was downloaded from https://www.ngdc.noaa.gov/eog/dmsp/downloadV4composites.html. We thank anonymous reviewers and the editors for their constructive comments which has improved this manuscript.

Appendix A. Supplementary data

Supplementary data to this article can be found online at https://doi.org/10.1016/j.rse.2018.11.038.

References

Adrian, R., O'Reilly, C.M., Zagarese, H., Baines, S.B., Hessen, D.O., Keller, W., Livingstone, D.M., Sommaruga, R., Straile, D., Van Donk, E., 2009. Lakes as sentinels of climate change. Limnol. Oceanogr. 54, 2283–2297.

Cao, Z., Duan, H., Feng, L., Ma, R., Xue, K., 2017. Climate- and human-induced changes in suspended particulate matter over Lake Hongze on short and long timescales. Remote Sens. Environ. 192, 98–113.

Carroll, M.L., Townshend, J.R., Dimiceli, C.M., Noojipady, P., Sohlberg, R.A., 2009. A new global raster water mask at 250 m resolution. Int. J. Digital Earth 2, 291–308.

Dai, Z., Hu, Y., Zhao, G., 2017. The suitability of different nighttime light data for GDP estimation at different spatial scales and regional levels. Sustainability 9, 305.

Deng, H., Chen, Y., 2017. Influences of recent climate change and human activities on water storage variations in Central Asia. J. Hydrol. 544, 46–57.

Donchyts, G., Baart, F., Winsemius, H., Gorelick, N., Kwadijk, J., van de Giesen, N., 2016. Earth's surface water change over the past 30 years. Nat. Clim. Chang. 6, 810–813.

Duan, A., Xiao, Z., 2015. Does the climate warming hiatus exist over the Tibetan Plateau? Sci. Rep. 5, 13711.

Feng, L., Hu, C., Chen, X., Zhao, X., 2013. Dramatic inundation changes of China's two largest freshwater lakes linked to the three gorges dam. Environ. Sci. Technol. 47, 9628–9634.

Feng, J., Qi, S., Liao, F., Zhang, X., Wang, D., 2015. Hydrological and sediment effects from sand mining in Poyang Lake during 2001–2010. Acta Geograph. Sin. 70, 837–845.

Feng, L., Han, X., Hu, C., Chen, X., 2016. Four decades of wetland changes of the largest freshwater lake in China: possible linkage to the Three Gorges Dam? Remote Sens. Environ. 176, 43–55.

Feng, M., Sexton, J.O., Channan, S., Townshend, J.R., 2016. A global, high-resolution (30-m) inland water body dataset for 2000: first results of a topographic–spectral classification algorithm. Int. J. Digital Earth 9, 113–133.

Feyisa, G.L., Meilby, H., Fensholt, R., Proud, S.R., 2014. Automated Water Extraction Index: a new technique for surface water mapping using Landsat imagery. Remote Sens. Environ. 140, 23–35.

Fisher, A., Flood, N., Danaher, T., 2016. Comparing Landsat water index methods for automated water classification in eastern Australia. Remote Sens. Environ. 175, 167–182.

Fujita, K., Sakai, A., Nuimura, T., Yamaguchi, S., Sharma, R.R., 2009. Recent changes in Imja Glacial Lake and its damming moraine in the Nepal Himalaya revealed by in situ surveys and multi-temporal ASTER imagery. Environ. Res. Lett. 4, 045205.

Gao, Y., Leung, L.R., Zhang, Y., Cuo, L., 2015. Changes in moisture flux over the Tibetan Plateau during 1979–2011: insights from a high-resolution simulation. J. Clim. 28, 4185–4197.

Gong, P., Niu, Z., Cheng, X., Zhao, K., Zhou, D., Guo, J., Liang, L., Wang, X., Li, D., Huang, H., Wang, Y., Wang, K., Li, W., Wang, X., Ying, Q., Yang, Z., Ye, Y., Li, Z., Zhuang, D., Chi, Y., Zhou, H., Yan, J., 2010. China's wetland change (1990–2000) determined by remote sensing. Sci. China Earth Sci. 53, 1036–1042.

Han, Q., Zhang, S., Huang, G., Zhang, R., 2016. Analysis of long-term water level variation in Dongting Lake, China. Water 8, 306.

Huang, Q., Zhang, Y., Chen, W., Huang, Y., 2007. Variation of hydrological characteristics of Tianmu Lake and its effect on the Tianmuhu wetland and ecological environment of the Tianmu Lake. Wetland Sci. 5, 51–57.

Ji, L., Zhang, L., Wylie, B., 2009. Analysis of dynamic thresholds for the normalized difference water index. Photogramm. Eng. Remote. Sens. 75, 1307–1317.

Lehner, B., Döll, P., 2004. Development and validation of a global database of lakes, reservoirs and wetlands. J. Hydrol. 296, 1–22.

Li, G., Lin, H., 2017. Recent decadal glacier mass balances over the Western Nyainqentanglha Mountains and the increase in their melting contribution to Nam Co Lake measured by differential Bistatic SAR interferometry. Glob. Planet. Chang. 149, 177–190.

Li, J., Sheng, Y., 2012. An automated scheme for glacial lake dynamics mapping using Landsat imagery and digital elevation models: a case study in the Himalayas. Int. J. Remote Sens. 33, 5194–5213.

Li, X., Li, A., Liu, G., Jiang, J., 2010. Spatial distribution pattern of the lakes in the Yunan-Guizhou Plateau. In: Resource and Environment in the Yangtze Basin. 19. pp. 90–96.

Li, W., Du, Z., Ling, F., Zhou, D., Wang, H., Gui, Y., Sun, B., Zhang, X., 2013. A comparison of land surface water mapping using the normalized difference water index from TM, ETM+ and ALI. Remote Sens. 5, 5530–5549.

Li, N., Liu, J., Wang, Z., 2014. Dynamics and driving force of lake changes in Northeast China during 2000–2010. J. Lake Sci. 26, 545–551.

Li, B., Zhang, J., Yu, Z., Liang, Z., Chen, L., Acharya, K., 2017. Climate change driven water budget dynamics of a Tibetan inland lake. Glob. Planet. Chang. 150, 70–80.

Ma, R., Duan, H., Hu, C., Feng, X., Li, A., Ju, W., Jiang, J., Yang, G., 2010. A half-century of changes in China's lakes: global warming or human influence? Geophys. Res. Lett. 37, L24106.

Ma, R., Yang, G., Duan, H., Jiang, J., Wang, S., Feng, X., Li, A., Kong, F., Xue, B., Wu, J., Li, S., 2011. China's lakes at present: number, area and spatial distribution. Sci. China Earth Sci. 54, 283–289.

Ma, S., Zhou, T., Dai, A., Han, Z., 2015. Observed changes in the distributions of daily precipitation frequency and amount over China from 1960 to 2013. J. Clim. 28, 6960–6978.

Mao, D., Wang, Z., Wu, J., Wu, B., Zeng, Y., Song, K., Yi, K., Luo, L., 2018. China's wetlands loss to urban expansion. Land Degrad. Dev. 29, 2644–2657.

McFeeters, S.K., 1996. The use of the normalized difference water index (NDWI) in the delineation of open water features. Int. J. Remote Sens. 17, 1425–1432.

McFeeters, S., 2013. Using the normalized difference water index (NDWI) within a geographic information system to detect swimming pools for mosquito abatement: a practical approach. Remote Sens. 5, 3544–3561.

Niu, Z., Zhang, H., Wang, X., Yao, W., Zhou, D., Zhao, K., Zhao, H., Li, N., Huang, H., Li, C., Yang, J., Liu, C., Liu, S., Wang, L., Li, Z., Yang, Z., Qiao, F., Zheng, Y., Chen, Y., Sheng, Y., Gao, X., Zhu, W., Wang, W., Wang, H., Weng, Y., Zhuang, D., Liu, J., Luo, Z., Cheng, X., Guo, Z., Gong, P., 2012. Mapping wetland changes in China between 1978 and 2008. Chin. Sci. Bull. 57, 2813–2823.

Otsu, N., 1979. A threshold selection method from gray-level histograms. IEEE Trans. Syst. Man Cybern. 9, 62–66.

Pekel, J.-F., Cottam, A., Gorelick, N., Belward, A.S., 2016. High-resolution mapping of global surface water and its long-term changes. Nature 540, 418–422.

Peng, D., Zhou, T., 2017. Why was the arid and semiarid Northwest China getting wetter in the recent decades? J. Geophys. Res. 122, 9060–9075.

Piao, S., Ciais, P., Huang, Y., Shen, Z., Peng, S., Li, J., Zhou, L., Liu, H., Ma, Y., Ding, Y., Friedlingstein, P., Liu, C., Tan, K., Yu, Y., Zhang, T., Fang, J., 2010. The impacts of climate change on water resources and agriculture in China. Nature 467, 43–51.

Ray, D.K., Gerber, J.S., MacDonald, G.K., West, P.C., 2015. Climate variation explains a third of global crop yield variability. Nat. Commun. 6, 5989.

Salerno, F., Thakuri, S., D'Agata, C., Smiraglia, C., Manfredi, E.C., Viviano, G., Tartari, G., 2012. Glacial lake distribution in the Mount Everest region: uncertainty of measurement and conditions of formation. Glob. Planet. Chang. 92–93, 30–39.

Salerno, F., Gambelli, S., Viviano, G., Thakuri, S., Guyennon, N., D'Agata, C., Diolaiuti, G., Smiraglia, C., Stefani, F., Bocchiola, D., Tartari, G., 2014. High alpine ponds shift upwards as average temperatures increase: a case study of the Ortles–Cevedale mountain group (southern Alps, Italy) over the last 50years. Glob. Planet. Chang. 120, 81–91.

Salerno, F., Thakuri, S., Guyennon, N., Viviano, G., Tartari, G., 2016. Glacier melting and precipitation trends detected by surface area changes in Himalayan ponds. Cryosphere 10, 1433–1448.

Schneider, U., Becker, A., Finger, P., Meyer-Christoffer, A., Ziese, M., Rudolf, B., 2014. GPCC's New Land Surface Precipitation Climatology Based on Quality-controlled in Situ Data and Its Role in Quantifying the Global Water Cycle. vol. 115.

Shi, C., 1989. A General Outline of Chinese Lakes. Science press, Beijing.

Shi, P., Sun, S., Wang, M., Li, N., Wang, J.A., Jin, Y., Gu, X., Yin, W., 2014. Climate change regionalization in China (1961–2010). Sci. China Earth Sci. 57, 2676–2689.

Smith, L.C., Sheng, Y., MacDonald, G.M., Hinzman, L.D., 2005. Disappearing Arctic Lakes. Science 308, 1429.

Smol, J.P., Douglas, M.S.V., 2007. Crossing the final ecological threshold in high Arctic ponds. Proc. Natl. Acad. Sci. 104, 12395–12397.

Song, C., Huang, B., Richards, K., Ke, L., Hien, V.P., 2014. Accelerated lake expansion on the Tibetan Plateau in the 2000s: induced by glacial melting or other processes? Water Resour. Res. 50, 3170–3186.

Sun, F., Zhao, Y., Gong, P., Ma, R., Dai, Y., 2014. Monitoring dynamic changes of global land cover types: fluctuations of major lakes in China every 8 days during 2000 − 2010. Chin. Sci. Bull. 59, 171–189.
Tao, S., Fang, J., Zhao, X., Zhao, S., Shen, H., Hu, H., Tang, Z., Wang, Z., Guo, Q., 2015. Rapid loss of lakes on the Mongolian Plateau. Proc. Natl. Acad. Sci. 112, 2281–2286.
Tong, K., Su, F., Xu, B., 2016. Quantifying the contribution of glacier-melt water in the expansion of the largest lake in Tibet. J. Geophys. Res. 121, 11158–11173.
Tong, Y., Zhang, W., Wang, X., Couture, R.-M., Larssen, T., Zhao, Y., Li, J., Liang, H., Liu, X., Bu, X., He, W., Zhang, Q., Lin, Y., 2017. Decline in Chinese lake phosphorus concentration accompanied by shift in sources since 2006. Nat. Geosci. 10, 507–511.
Verpoorter, C., Kutser, T., Seekell, D.A., Tranvik, L.J., 2014. A global inventory of lakes based on high-resolution satellite imagery. Geophys. Res. Lett. 41, 6396–6402.
Wan, W., Long, D., Hong, Y., Ma, Y., Yuan, Y., Xiao, P., Duan, H., Han, Z., Gu, X., 2016. A lake data set for the Tibetan Plateau from the 1960s, 2005, and 2014. Sci. Data 3, 160039.
Wang, S., Dou, H., 1998. Chinese Lakes Inventory. Science Press, Beijing, China.
Wang, X., Ding, Y., Liu, S., Jiang, L., Wu, K., Jiang, Z., Guo, W., 2013. Changes of glacial lakes and implications in Tian Shan, Central Asia, based on remote sensing data from 1990 to 2010. Environ. Res. Lett. 8, 044052.
Wang, J., Sheng, Y., Tong, T.S.D., 2014. Monitoring decadal lake dynamics across the Yangtze Basin downstream of Three Gorges Dam. Remote Sens. Environ. 152, 251–269.
Wang, L., Hu, Q., Hu, Y., Wang, Y., Lin, H., 2016. Changes and cause analysis of water level characteristic factors in Taihu Lake during period from 1954 to 2013. J. Hohai Univ. (Nat. Sci.) 44, 13–19.
Wang, R., Li, Z., Zhao, G., Tan, Z., Li, Y., 2017. Characteristics of the evolution of hydrological regimes across the Poyang Lake region in the past 60 years. Trop. Geogr. 37, 512–521.
Wang, X.I.N., Chai, K., Liu, S., Wei, J., Jiang, Z., Liu, Q., 2017. Changes of glaciers and glacial lakes implying corridor-barrier effects and climate change in the Hengduan Shan, southeastern Tibetan Plateau. J. Glaciol. 63, 535–542.
Wang, L., Henderson, M., Liu, B., Shen, X., Chen, X., Lian, L., Zhou, D., 2018. Maximum and minimum soil surface temperature trends over China, 1965–2014. J. Geophys. Res. Atmos. 123, 2004–2016.
Wen, Y., Huang, L., Luo, L., 2006. Analysis of water level variation in Hongze Lake. In: Water Resources of Jiangsu, pp. 27–28.
Wood, J., 1996. The Geomorphological Characterisation of Digital Elevation Models. University of Leicester, Department of Geography, Leicester, UK.
Wu, J., He, S., Peng, J., Li, W., Zhong, X., 2013. Intercalibration of DMSP-OLS night-time light data by the invariant region method. Int. J. Remote Sens. 34, 7356–7368.
Wurtsbaugh, W.A., Miller, C., Null, S.E., Derose, R.J., Wilcock, P., Hahnenberger, M., Howe, F., Moore, J., 2017. Decline of the world's saline lakes. Nat. Geosci. 10, 816–821.
Xu, H., 2006. Modification of normalised difference water index (NDWI) to enhance open water features in remotely sensed imagery. Int. J. Remote Sens. 27, 3025–3033.
Xu, Y., Xu, X., Tang, Q., 2016. Human activity intensity of land surface: concept, methods and application in China. J. Geogr. Sci. 26, 1349–1361.
Yamazaki, D., Trigg, M.A., Ikeshima, D., 2015. Development of a global ~90 m water body map using multi-temporal Landsat images. Remote Sens. Environ. 171, 337–351.
Yang, X., Lu, X., 2014. Drastic change in China's lakes and reservoirs over the past decades. Sci. Rep. 4, 6041.
Yang, K., Ye, B., Zhou, D., Wu, B., Foken, T., Qin, J., Zhou, Z., 2011. Response of hydrological cycle to recent climate changes in the Tibetan Plateau. Clim. Chang. 109, 517–534.
Yang, K., Lu, H., Yue, S., Zhang, G., Lei, Y., La, Z., 2018. Quantifying recent precipitation change and predicting lake expansion in the Inner Tibetan Plateau. Clim. Chang. 147, 149–163.
Yu, J., Zhang, G., Yao, T., Xie, H., Zhang, H., Ke, C., Yao, R., 2016. Developing daily cloud-free snow composite products from MODIS Terra-Aqua and IMS for the Tibetan Plateau. IEEE Trans. Geosci. Remote Sens. 54, 2171–2180.
Zhang, G., Yao, T., Xie, H., Kang, S., Lei, Y., 2013. Increased mass over the Tibetan Plateau: from lakes or glaciers? Geophys. Res. Lett. 40, 2125–2130.
Zhang, G., Yao, T., Xie, H., Wang, W., Yang, W., 2015. An inventory of glacial lakes in the Third Pole region and their changes in response to global warming. Glob. Planet. Chang. 131, 148–157.
Zhang, G., Li, J., Zheng, G., 2017a. Lake-area mapping in the Tibetan plateau: an evaluation of data and methods. Int. J. Remote Sens. 38, 742–772.
Zhang, G., Yao, T., Piao, S., Bolch, T., Xie, H., Chen, D., Gao, Y., O'Reilly, C.M., Shum, C.K., Yang, K., Yi, S., Lei, Y., Wang, W., He, Y., Shang, K., Yang, X., Zhang, H., 2017b. Extensive and drastically different alpine lake changes on Asia's high plateaus during the past four decades. Geophys. Res. Lett. 44, 252–260.
Zhang, G., Yao, T., Shum, C.K., Yi, S., Yang, K., Xie, H., Feng, W., Bolch, T., Wang, L., Behrangi, A., Zhang, H., Wang, W., Xiang, Y., Yu, J., 2017c. Lake volume and groundwater storage variations in Tibetan Plateau's endorheic basin. Geophys. Res. Lett. 44, 5550–5560.
Zhou, J., Wang, L., Zhang, Y., Guo, Y., Li, X., Liu, W., 2015. Exploring the water storage changes in the largest lake (Selin Co) over the Tibetan Plateau during 2003–2012 from a basin-wide hydrological modeling. Water Resour. Res. 51, 8060–8086.
Zou, Z., Xiao, X., Dong, J., Qin, Y., Doughty, R.B., Menarguez, M.A., Zhang, G., Wang, J., 2018. Divergent trends of open-surface water body area in the contiguous United States from 1984 to 2016. Proc. Natl. Acad. Sci. 115, 3810–3815.